

FABRICATION, FILLING, SEALING AND TESTING OF  
MICRO HEAT PIPES

Except where reference is made to the work of others, the work described in this thesis is my own or was done in collaboration with my advisory committee. This thesis does not include proprietary or classified information.

---

Omkar Satish Nadgauda

Certificate of Approval:

---

Jay M. Khodadadi  
Professor  
Mechanical Engineering

---

Daniel K. Harris, Chair  
Associate Professor  
Mechanical Engineering

---

Bogdan Wilamowski  
Professor  
Electrical and Computer Engineering

---

Stephen L. McFarland  
Dean  
Graduate School

FABRICATION, FILLING, SEALING AND TESTING OF  
MICRO HEAT PIPES

Omkar Satish Nadgauda

A Thesis

Submitted to

the Graduate Faculty of

Auburn University

in Partial Fulfillment of the

Requirements for the

Degree of

Master of Science

Auburn, Alabama  
December 15, 2006

FABRICATION, FILLING, SEALING AND TESTING OF  
MICRO HEAT PIPES

Omkar Satish Nadgauda

Permission is granted to Auburn University to make copies of this thesis at its discretion, upon request of individuals or institutions and at their expense. The author reserves all publication rights.

---

Signature of Author

---

Date of Graduation

## VITA

Omkar Satish Nadgauda, son of Satish K. Nadgauda and Rajani S. Nadgauda, was born on January 9, 1982 in Pune, Maharashtra, India. He finished his high school education from Loyola College, Pune, Maharashtra, India in 2000. In August 2000, he entered the PVG's College of Engineering and Technology at University of Pune, Maharashtra, India and earned the degree of Bachelor of Mechanical Engineering in 2004 with a first class. He then entered the Graduate School at Auburn University in fall 2004.

THESIS ABSTRACT  
FABRICATION, FILLING, SEALING AND TESTING OF  
MICRO HEAT PIPES

Omkar Satish Nadgauda

Master of Science, December 15, 2006  
(B.E. Mech. PVG's COET, University of Pune, 2000)

99 Typed Pages

Directed by Daniel K. Harris

Micro heat pipes are small and passive heat transfer devices. Research is going on in its applications ranging from using them in high powered electronic devices to using them during brain surgeries. A combination of silicon with many different liquids as working fluids is being investigated. This thesis investigates the fabrication of micro heat pipes arrays and the possibility of using mercury as one of the working fluids. Water was also tried on some of them. A new sealing technique was used to seal the micro heat pipes filled with mercury. Tests were carried out on these charged devices and silicon dummies under an infra red camera. The results of the charged devices were compared with silicon dummy to check their working feasibility. The micro fabrication, charging, sealing and testing procedures are discussed in the following work. The results obtained from the tests conducted are also presented.

## ACKNOWLEDGEMENTS

I would like to acknowledge the San Diego Composites Corporation for providing the funding.

I would like to thank my advisor, Dr. Daniel K. Harris for his guidance and suggestions throughout this research. I would also like to thank Charles Ellis and Dr. Robert Dean for their valuable help and suggestions. I am also thankful to Bhavin Vadgama, Ashish Palkar, Abhisekh Dawre and Dr. Jeffrey Suhling for their help during fabrication and testing.

Most importantly, I am very grateful to my parents and brother whose unconditional support throughout my education has motivated me to go forward in my life and has brought me where I am.

Style manual or journal used IEEE

Computer software used Microsoft Office 2003, Solid Edge V17, LASI CAD,

## TABLE OF CONTENTS

LIST OF FIGURES .....	X
LIST OF TABLES .....	XIII
CHAPTER 1 MICRO HEAT PIPES .....	1
1.1 Introduction .....	1
1.2 Micro Heat Pipes .....	1
1.3 Operation .....	4
1.4 Operating Limits .....	5
1.4.1 Capillary Limit .....	5
1.4.2 Boiling Limit .....	5
1.4.3 Vapor Continuum Limitation .....	6
CHAPTER 2 LITERATURE REVIEW .....	8
CHAPTER 3 FABRICATION OF MICRO HEAT PIPES .....	29
3.1 Introduction .....	29
3.2 Design and dimensions of the micro heat pipes .....	29
3.3 Fabrication of channels .....	30
3.3.1 Cleaning of the wafer .....	30
3.3.2 Dehydration bake and Hexamethyldisilazane (HMDS) .....	31
3.3.3 Photoresist application .....	31
3.3.4 Soft bake and hard bake .....	33
3.3.5 Mask Alignment and Developing .....	33
3.3.6 E-beam deposition and Ultrasonic strip off .....	38
3.3.7 Ultrasonic photoresist strip off .....	39
3.3.8 Repeat procedure from Dehydration bake to Developing .....	40
3.3.9 Etching .....	42
3.3.10 Deposition of Ti/Pt/Au and Photoresist Removal .....	43
3.3.11 Dicing .....	46
3.4 Fabrication of the lids .....	46
3.4.1 Oxidation .....	47



3.4.2 Repeating the Procedures.....	48
3.4.3 Argon ion In-on-Au In ablation .....	54
3.4.4 Fabrication of Sensors and grooves .....	54
CHAPTER 4 TESTING AND RESULTS .....	62
4.1 Introduction .....	62
4.2 Charging.....	62
4.2.1 Charging of Mercury .....	62
4.2.2 Charging of water.....	65
4.3 Sealing.....	66
4.3.1 Cleaning of lids.....	66
4.3.2 Sealing of mercury micro heat pipes .....	66
4.3.3 Sealing of water micro heat pipes .....	68
4.3.4 Bonding technique used .....	69
4.4 Testing .....	69
4.4.1 Board.....	70
4.4.2 Experiments .....	71
4.4.3 Results.....	73
4.4.4 Conclusion .....	79
CHAPTER 5 DISCUSSION .....	82
5.1 Overview .....	82
5.2 Future work .....	83
BIBLIOGRAPHY.....	84

## LIST OF FIGURES

Figure 1.1: Micro heat pipe array on a silicon wafer. (100 $\mu\text{m}$ x 100 $\mu\text{m}$ x 9500 $\mu\text{m}$ ).....	3
Figure 1.2: Operation of a triangular cross section Micro heat pipe as show by G.P. Peterson [3] .....	4
Figure 2.1: Cross sections of heat pipes used by Launay et al (a) with triangular channels (2 wafers) and (b) triangular channels with arteries (3 wafers) [5].....	10
Figure 2.2: Proposed design of micro heat pipes in radiator fin by Bassam et al[6]. .....	14
Figure 2.3: Proposed vapor deposited micro heat pipes by Mallik et al.[10] .....	18
Figure 2.4: Micro heat pipe array tested by Wang et al. [11].....	20
Figure 3.1 : Wafer with negative photoresist.....	32
Figure 3.2 : Channel's mask (44 dies).....	35
Figure 3.3 : Single Die (22 channels; 100 microns x 9500 microns) .....	36
Figure 3.4 : Alignment of mask.....	37
Figure 3.5 : Developed photoresist.....	37
Figure 3.6 : Position of Ti/Ni/In layer.....	38
Figure 3.7 : Surface after the ultrasonic strip off.....	39
Figure 3.8 : Application of the positive photoresist .....	41

Figure 3.9 : Wafer after developing .....	41
Figure 3.10 : etched wafer .....	43
Figure 3.11 : Mercury on a Ti/Pt/Au wafer .....	44
Figure 3.12 : Wafer after Ti/Pt/Au deposition .....	45
Figure 3.13 : Channel wafer after all the procedures. ....	45
Figure 3.14 : Double side polished wafer on both sides of the wafer .....	47
Figure 3.15 : Wafer after application of photoresist and exposure and developing of first mask .....	49
Figure 3.16 : Deposition of Ti/Pt/Au layer and photoresist strip off.....	50
Figure 3.17 : Application of negative photoresist .....	51
Figure 3.18 : Wafer after exposing to mask 2 and developing. Saw tape is also put on the back side of wafer to protect that surface while buffer oxide etch processes. ....	51
Figure 3.19 : Buffer oxide etch processes. ....	52
Figure 3.20 : DRIE.....	52
Figure 3.21 : Application of Ti/Cu Layer .....	53
Figure 3.22 : Photoresist strip off. ....	53
Figure 3.23 : Indium plating (10 $\mu\text{m}$ ) .....	54
Figure 3.24 : Application of positive photoresist and exposing the sensor mask. ...	56
Figure 3.25 : Developed photoresist and Ti/Pt/Au deposition.....	56
Figure 3.26 : Wafer with sensor trace. ....	57
Figure 3.27 : Sensor mask (5 sensors per die) .....	58

Figure 3.28 : Single die (5 sensors) .....	59
Figure 3.29 : Sensor serpentine .....	60
Figure 3.30 : Final assembly .....	61
Figure 4.1: Setup used to fill micro heat pipes. The picture shows a test dummy being filled.....	63
Figure 4.2 : Filling of Mercury in the channels.....	64
Figure 4.3: TV screen attached to microprobe station showing mercury in the channels.....	65
Figure 4.4 : crocodile clip and micro heat pipes. ....	67
Figure 4.5: Vacuum chamber used to seal the micro heat pipes.....	68
Figure 4.6 : LCP board with micro heat pipes and lead and heating wires on it...	70
Figure 4.7 : Experimental setup.....	71
Figure 4.8 : Schematic Diagram of testing apparatus.....	72
Figure 4.9 : Numbering of the sensors .....	74
Figure 4.10 : Graphical representation of Si dummy results.....	76
Figure 4.11 : Infra red image of micro heat pipes at a power of 2.37 W. ....	76
Figure 4.12 : Graphical representation of water-filled mciro heat pipes .....	77
Figure 4.13 : Graphical representation of mercury-filled micro heat pipes .....	79
Figure 4.14 : Graphical representation of the comparable results .....	80

## LIST OF TABLES

Table 4.1: Test results for Si dummy.....	75
Table 4.2 : Test results for water-filled micro heat pipes .....	77
Table 4.3 : Test results for mercury-filled micro heat pipes .....	79
Table 4.4 : Comparable results .....	80

# CHAPTER 1

## MICRO HEAT PIPES

### 1.1 Introduction

In the recent technological boom, the electronic equipments are becoming smaller and faster. This generates a large quantity of heat, so there has been a lot of recent emphasis on heat dissipation. Some devices generate as much as  $60 \text{ W/m}^2$  to  $100 \text{ W/m}^2$ [1] of heat; as a result electronic cooling is emerging as an important field. Space is one of the obstacles in the progress of electronic cooling techniques. The main aim is to provide as little resistance as possible in the thermal path [2].

The micro heat pipe is being looked at as one of the emerging technologies in thermal cooling: it helps in over all cooling of the electronic device and also results in uniform thermal distribution[1]. One of the prime advantages of micro heat pipe is its size. It has dimensions in microns and can be fabricated on the substrate itself. This helps in removing heat directly from a hotspot. It is a passive heat transfer device.

Micro heat pipes utilize the latent heat of vaporization of the fluid; this allows the micro heat pipes to carry large heat fluxes [2]. The use of different fluids can of course, change its working ability.

### 1.2 Micro Heat Pipes

The concept of the micro heat pipe was first introduced by Cotter in 1984 [3]. Cotter defined it as a pipe so small that the mean curvature of the liquid-vapor

interface is necessarily comparable in magnitude to the reciprocal of the hydraulic radius of the total flow channel[3]. The idea was to incorporate small micro heat pipes in semiconductor devices. This provided a more uniform distribution and thermal control[3]. More development has taken place since that time.

The micro heat pipe is a non circular channel having sharp edges which act as the capillaries as shown in fig. 1.1. Though the first idea was to apply these heat pipes in semiconductor devices, other uses have been investigated and proposed. Some of them include heat removal from laser diodes, thermal control of photovoltaic cells, thermal control of leading edge of hypersonic aircraft and medical applications such as nonsurgical treatment of cancer tissue by hyper or hypothermia [3].

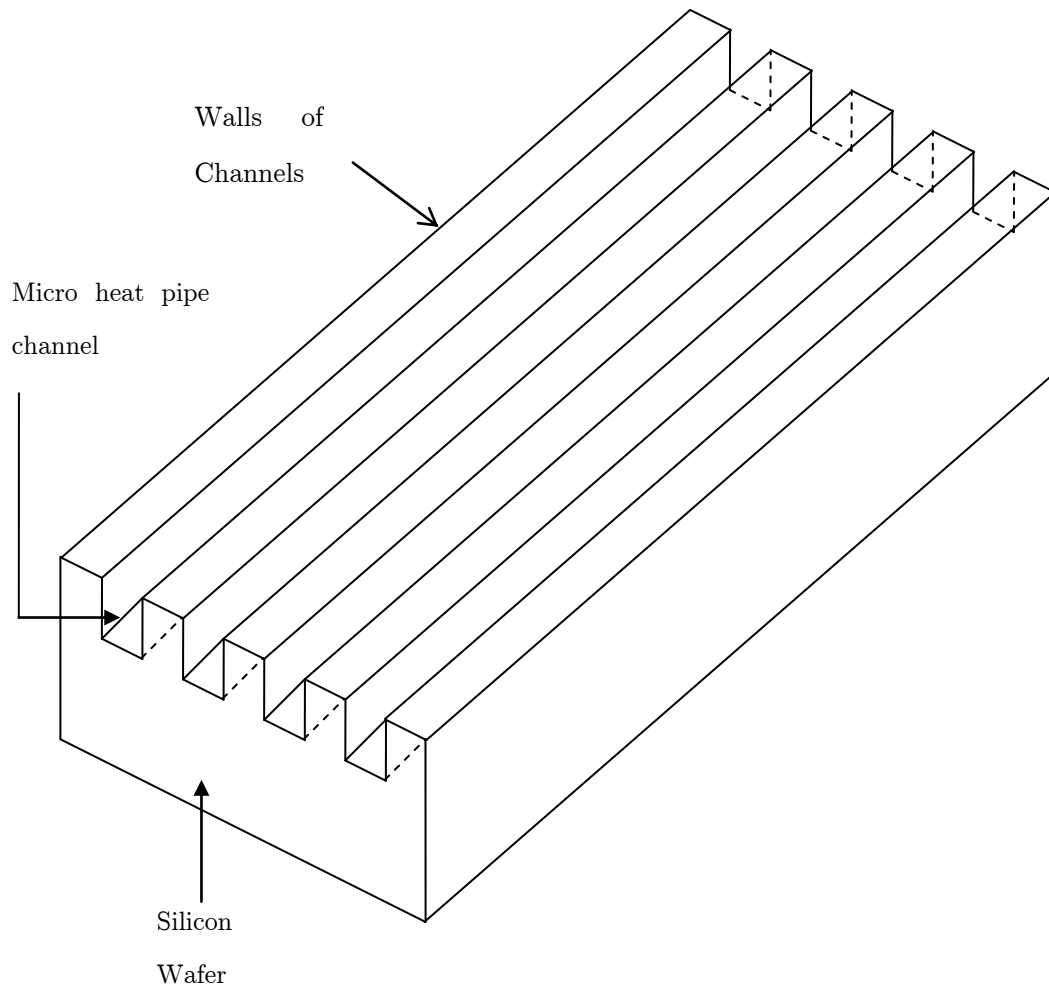


**Figure 1.1:** Micro heat pipe array on a silicon wafer. (100  $\mu\text{m}$  x 100  $\mu\text{m}$  x 9500  $\mu\text{m}$ )



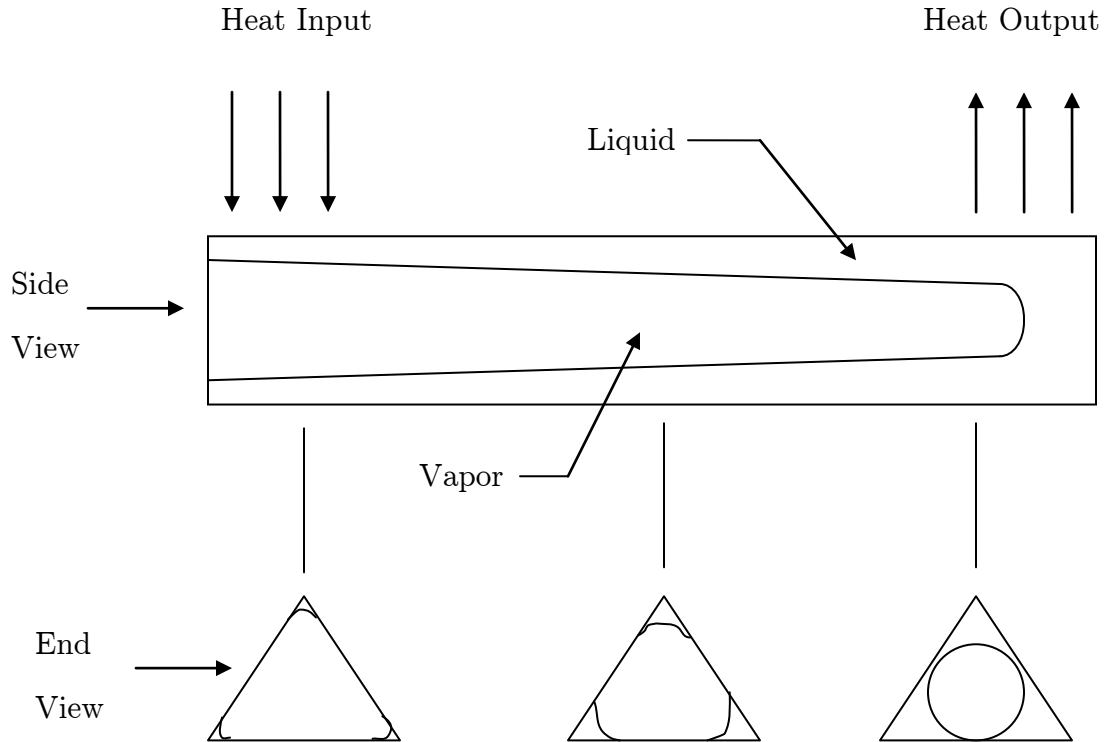


**Figure 1.2:** Operation of a triangular cross section Micro heat pipe as show by G.P. Peterson [3]

### 1.3 Operation

The operating principle of the micro heat pipe is in general the same as a larger and conventional heat pipe. Heat applied to one end vaporizes the working fluid which moves to the cooler end where it condenses and rejects heat. The vaporization and condensation process changes the liquid-vapor interface continuously in the edges. This gives rise to a pressure gradient along the evaporator and condensation region. This pressure difference causes the condensate to flow back to the evaporator section of the micro heat pipe. Since the edges act as capillaries there is no need for a wicking structure [cotter]. The operation is shown in fig. 1.2.

## 1.4 Operating Limits

The heat transport capacity of the micro heat pipe is governed by three primary limitations, capillary limit, boiling limit and vapor continuum limit. Modeling of a micro heat pipe is aimed at satisfying these limits. The maximum amount of heat transfer is limited by the lowest limits of the following [1].

### 1.4.1 Capillary Limit

The capillary limit is the most important governing limitation on micro heat pipes[1]. Capillary action causes the circulation of fluid within micro heat pipes from the condenser to the evaporator. The capillary limit plays a major role in low-temperature situations when the Capillary pressure difference is not enough to pump the fluid from condenser to evaporator [1]. The edges of a micro heat pipes act as wick. Dry out is caused when an excess of heat is supplied to the micro heat pipe above the capillary limit.

### 1.4.2 Boiling Limit

Heat is provided at the evaporator section of the micro heat pipe. In the case of high heat fluxes at high temperatures, incipience can be initiated. As more incipient sites become active, the bubbles coalesce together and form a vapor film over the wall [1]. This layer of vapor stops the liquid from reaching the evaporator section, and results in micro heat pipe burn out as the temperature of the wall increases. This limit rarely occurs for liquid metal heat pipes for high temperature operations [1].

The maximum heat flux related to boiling limit, according to Faghri [1] is given by

$$q_{crit} = \frac{k_l T_{crit}}{\delta} \quad (1)$$

Where,

$k_l$  = Thermal conductivity in dominant thin liquid film

$$T_{crit} = T_s - T_v,$$

$T_s$  = wall-liquid interface temperature,

$T_v$  = being the heat pipe temperature.

### 1.4.3 Vapor Continuum Limitation

The vapor continuum behavior disappears as the size of a micro heat pipe reaches a critical point [4]. The Knudsen number is used to define this criterion.

$$Kn = \frac{\lambda}{D} \quad (2)$$

where,

$\lambda$  = mean free path of the vapor

$D$  = vapor core diameter

$Kn$  = Knudsen number

If  $Kn$  is less than or equal to 0.01, the micro heat pipe will have a continuum flow. On the other hand if  $Kn$  is greater than 0.01 it is a case of rarefied or free molecular flow [4]. Heat transfer capacity is limited if we are in the rarefied or molecular flow region, and a large gradient is observed along the micro heat pipe length [4]. As the vapor space dimension ( $D$ ) goes down, the transition temperature sharply increases [4] and this increase in the transition temperature makes the startup of the micro heat pipe difficult [4]. If the transition temperature of the working fluid is higher than the working temperature, the working fluid is not good for the working conditions [4]. If an electronic device starts from room temperature,

it will experience a rarefied flow stage in which there will be a higher temperature gradient along the axial direction (until the transition temperature is surpassed).

## CHAPTER 2

### LITERATURE REVIEW

In the following chapter, we have a look at some previous works regarding fabrication of micro heat pipes. Focus is also given on testing methods and results obtained by some of the works.

In 1993, Gerner et al. studied silicon water micro heat pipes [2]. Micro heat pipes were fabricated on a double sided polished silicon wafer with  $\langle 100 \rangle$  crystallographic orientation. The wafer was 50.8 mm (2 inches) in diameter and 280 microns thick and triangular in cross section to improve wicking [2]. They were 25.4 mm long, 100 microns wide and 70.72 micron deep. They were spaced 100 microns apart and, there were 125 of them on one wafer.

First the wafer went a dry-wet-dry oxidation process, followed by spinning of photoresist and masking and exposing the pattern. The exposed photoresist was then selectively etched by Hydrofluoric acid (HF) solution. An anisotropic wet-chemical etching was carried out on open Silicon windows; this etching was also used to create a reservoir and a trough hole at the condenser end to fill and evacuate the micro heat pipes. To supply the heat a resistive heater was fabricated over the evaporator section and small scale P-N junctions were fabricated on the opposite side of the wafer to measure the temperatures. Boron and phosphorus diffusion was used to create P-N junctions oriented along the axis. At constant current, the voltage varied linearly with temperature. The sensitivity was 2 to 3 mV/ °C. Finally a 20 mils thick 7400 Pyrex glass was electrostatically bonded.

The testing was carried out in a controlled environment. The pipes were evacuated before filling the fluid. A known heat input was supplied through the heater which was 280 mm long. The condenser was cooled by running water. The heat input was calculated from the resistance and voltage drop across the element using the Ohm's law. Three of the pipes, one on each side and one in the middle, were observed. Forward bias was applied across the diodes to get a linear variation of voltage against temperature. The tests were conducted at atmospheric conditions. They observed that as the heat input was increased from 0.1 W to 0.9 W for deionized water filled micro heat pipes, the effective conductivity increased from 347.5 W/m°C to 580.9 W/m°C, respectively, and the heat flux increased from 1.406 W/cm<sup>2</sup> to 12.654 W/cm<sup>2</sup>. The temperature distribution was assumed to be one-dimensional [2]. A model was also created for specific thermal conductivity, the ratio of effective thermal conductivity to the density of fluid. With the help of the model, fluids like mercury and potassium on silicon surface were found to have specific conductivity of 224,517 and 55,040 (W/m°C) (g/cm<sup>3</sup>) respectively.

Launay et al. [5] tried to fabricate and test micro heat pipes with arteries, and normal, triangular-shaped micro heat pipes. Ethanol and methanol were used as working fluids. The micro heat pipe array was 20mm x 20mm and the condenser section was designed the same as done by Gerner et al.[2].

They followed two designs one for the normal triangular geometry and the another for the arteries for flow of liquid from the condenser section to the evaporator section as shown in fig. 2.1. The first one had 55 parallel triangular channels, which were 270 microns wide and 170 microns deep. They were spaced at a distance of 130 microns each and were 20mm in length. Anisotropic wet chemical etching was used to fabricate the channels. The device was hermetically closed by bonding a plain silicon wafer with the first one.

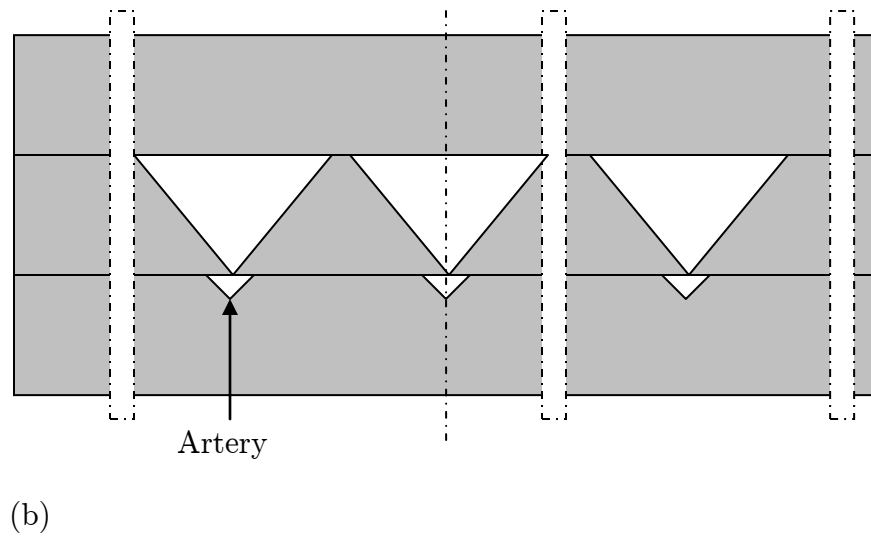
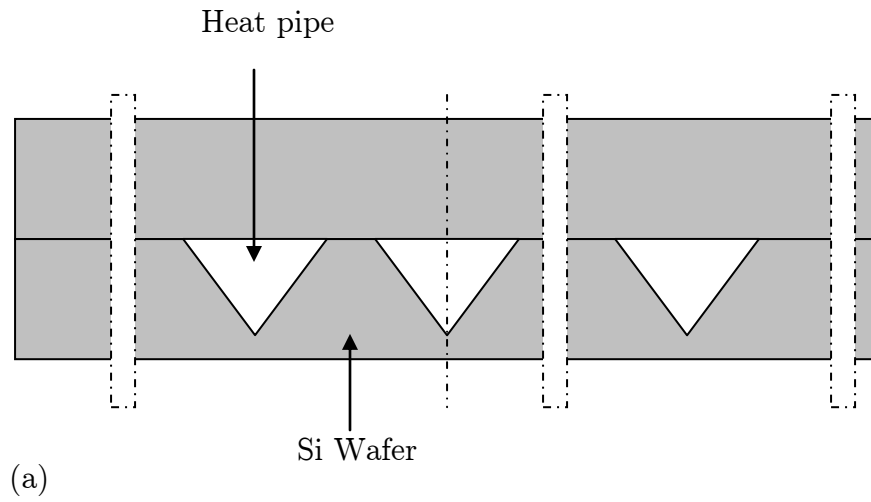


**Figure 2.1:** Cross sections of heat pipes used by Launay et al (a) with triangular channels (2 wafers) and (b) triangular channels with arteries (3 wafers) [5].

The second design had arteries to separate liquid and vapor flow. Three wafers were used to fabricate the design. In the middle wafer 25 triangular shaped grooves 500 microns wide and 320 microns apart were etched. On the bottom wafer 25 smaller triangular grooves were etched, placed as shown in fig. 2.1. The top most wafer was used to seal the device. The wafers used were 50.8mm (2 inch) in diameter. The orientation was  $\langle 100 \rangle$ . Fabrication followed the usual steps of oxide growth followed by spinning and exposing. Then the exposed silicon was etched using a 40 wt. % aqueous KOH solution maintained at 60°C [2, 5].

Silicon was used instead of Pyrex glass to seal the device, to get more uniform distribution from the heaters [5]. Si-Si bonding is the most intimate bonding without the use of external forces [5]. Before the bonding the oxide on the wafers was removed by dipping the wafers in HF solution. It was followed by piranha ( $\text{H}_2\text{SO}_4:\text{H}_2\text{O}_2$ ) and RCA ( $\text{NH}_4\text{OH}:\text{H}_2\text{O}_2:\text{H}_2\text{O}$ ) for 15 minutes each to remove the organic and metallic surface contamination. This made the Si surface hydrophilic [5]. The wafers were then bonded at room temperature followed by annealing for 1 hour at 1100°C to get a strong bond.

Fluid solidification in a vacuum was implemented in order to eliminate non-condensable gases from the micro heat pipe system. The fluid was evaporated to release non-condensable gases, and the fluid solidified in a vessel dipped in liquid nitrogen. It followed by the evacuation of non-condensable gases by the help of a vacuum pump. For the micro heat pipe arrays, working fluid, which was vaporized in the heated vessel, was introduced in the cooled micro heat pipes arrays, where it got condensed. The charge was measured by pressure and temperature measurements in a chamber where the charge was transferred after the experiment. Ethanol and methanol were used as working fluids since they were found suitable for range below 125°C [5].



During the experiments the amount of working fluid and the environmental conditions were changed in order to optimize the operation of micro heat pipe. The heat input was given by the poly silicon heater. The doping level was high in order to maintain a constant resistivity with respect to temperature. Temperature was measured by T-type thermocouple. Phosphorus was used for doping [5].

The results were obtained under the heat sink temperature of 30°C and a flow rate of 128 liters per hour. For the triangular channel micro heat pipe array, with the power of 3W and ethanol as a charge, the charged micro heat pipe array showed a slight decrease in temperature relative to the empty one. However due to experimental uncertainty, the heat transfer enhancement could not be clearly proved [5].

On the other hand a noticeable heat transfer enhancement was observed in the micro heat pipe arrays with arteries. For an input power of 2W, with the arteries either empty or filled with 50 % methanol, the temperature difference between evaporator and condenser section reached 4.7 K when an empty array was used, and it decreased to 1.6 K when a filled array was used [5].

Bassam et al [6] in 1993 showed that liquid metal micro heat pipes were far more effective than water-filled micro heat pipes. They studied liquid metal micro heat pipes for space applications. The aim of their study was to increase the ratio of thermal conductivity to density of the material (specific thermal conductivity) and enhance waste heat rejection in space [6]. The idea was to incorporate micro heat pipes in a fin made of silicon, as shown in fig. 2.2. The micro heat pipes would be either connected to conventional heat pipes running through the fins or the micro heat pipes will be made longer to work without the conventional heat pipes [6]. Up to the etching, the fabrication procedure for V-shaped grooves was same as Gerner et al.[2]. There was a proposed deviation in the procedure after that. A

coating of metals like chromium (Cr), titanium (Ti), Tungsten (W) or molybdenum (Mo) was to be deposited using procedures such as thermal evaporation, sputtering, CVD or electroplating, to avoid direct interaction of liquid metal with silicon [2]. Pyrex glass was used as a lid and the heater was fabricated into the silicon near the evaporator section using p-type (Boron) diffusion. A series of p-n junction diodes were imbedded to measure the temperature. They also developed a mathematical model to predict working of liquid metal micro heat pipes. A water filled micro heat pipe was used as prototype for the liquid metal micro heat pipes and the results from the model showed that with using liquid metal heat pipes the specific thermal conductivity can be increased 200 times over the Gr/Cu (graphite/copper) composite material.

Youngcheol, Kiet and Chang [7] tried to fabricate micro channels in a novel way. The fabrication process was designed in such a way that the overall cost of its fabrication on IC chip was very low compared to the contemporary processes. It was also able to integrate with the existing IC processes. It could be added at the end in IC chip fabrication process and hence eliminated the need to change the IC fabrication process [7]. The concept was to form a seed layer of chromium and nickel on to the <100> silicon wafer. Then a thick (10 $\mu$ m) layer of AZ 4620 photoresist was applied and exposed according to the pattern. Nickel electroplating was used to form the walls.

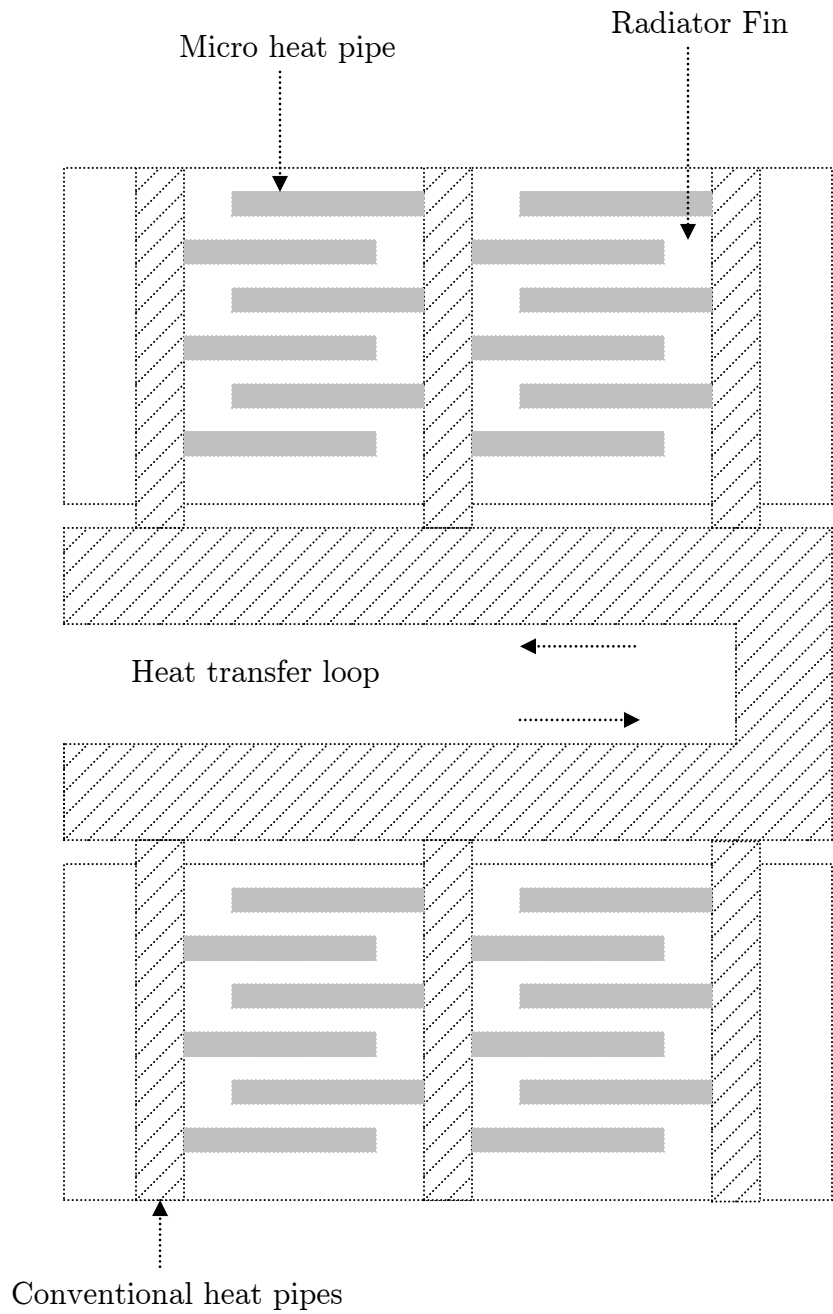


**Figure 2.2:** Proposed design of micro heat pipes in radiator fin by Bassam et al[6].

Electroplating occurred in the places where the photoresist was exposed. After some time the nickel walls formed an overhang over the photoresist walls. The wafer was then sprayed with acetone, which removed the photoresist from under the overhang. This was followed by an additional electroplating until the overhangs merged together and increased in height allowing for the creation of channels below the overhang. The heat removal rate was considerably low, which was the main disadvantage of this method. Also, this method could not be used to construct micro heat pipes until an effective way or process to seal the ends is discovered.

In 2003 Man Lee et al [8] fabricated a micro heat pipe system using a CMOS compatible method. The micro heat pipes were capped by a 0.5  $\mu\text{m}$  nitride membrane. They used glass to get a clear visualization of the two phase phenomena. Temperature micro sensors were fabricated and capacitors were used to measure the capacitance since the capacitance is directly proportional to the dielectric constant of the medium.

The heat pipes were formed on a  $\langle 100 \rangle$  silicon wafer by an etching process using a TMAH solution. The total device was 12 mm wide and 24 mm long and carried varied number of triangular heat pipes, 100 microns wide and 20 mm long. Local heater was used to generate heat. Temperature micro sensors were created using selectively doped silicon regions. The temperature sensors were buried under silicon to ensure measurement accuracy [8]. The huge difference between the dielectric constant of water and air was used to measure the void fraction which plays an important role in the heat transfer of two phase flows. The bottom capacitor electrode was created by heavily doping the V-groove and wafer back, and the top electrode was formed by sputtering a thin layer of metal over nitride or glass cover. The top electrode was kept as small as possible to obtain local void fraction. The parasitic capacitance is lower in glass as compared to nitride

membrane [8]. A silicon oxide layer on the silicon wafer acted as insulation between the top and bottom electrodes.

In their CMOS compatible process, a nitride film was deposited over the device wafer. The heater and temperature sensors were fabricated by selectively doping boron in n-wells formed by phosphorus implantation. After the formation of heaters, sensors and capacitors, the cover wafer was bonded on the device wafer by fusion bonding at 1050°C for 1 hour. The bonding was followed by dissolving the cover wafer in a TMAH solution, exposing the nitride layer. The V-grooves remained covered with nitride layer.

In the glass based fabrication process, the fabrication of the heaters, sensors and electrodes followed the same method as the CMOS compatible method. The bonding of glass and silicon wafer was done by die-by-die anodic bonding at 330°C at voltage of 700 V.

The same authors tested and characterized the above built micro heat pipe system [9]. They used two charging techniques. In the first, they filled the micro heat pipes through one charge hole in vacuum. After the micro heat pipe was filled, the hole was left open until the water evaporated and the desired amount of charge was left. Then the hole was sealed. In the second, they made two holes on a micro heat pipe, one at the condenser end and the other at the evaporator end and one hole was sealed. After the evaporation of a certain amount of charged water, the other hole was sealed. This system eliminated the need for a vacuum system.

The testing was carried out by attaching the microdevices on a Printed Circuit Board. The condenser side was cooled by a heat sink, and the measurements were done by connecting the data acquisition system with the board. The two phase flow was recorded by a CCD camera mounted on a microscope. The temperature decrease was almost linear with the distance from the heater. The

negative temperature gradient increased with an increase in power. The transition from vapor to liquid was visible under the camera. The evaporator had a void fraction of 1 while the condenser had a void fraction of 0. The void fraction increased along with the increase in power input.

A.K Mallik, G.P .Peterson and Mark H. Weichold fabricated a micro heat pipe array using a vapor deposition technique [10]. The work gave details of all the procedures used in fabricating the micro heat pipes arrays such as mask fabrication, oxidation etc. The grooves were fabricated by Orientation Dependent Etching (ODE) using a KOH-1-propanol-H<sub>2</sub>O. In order to close the grooves, Cu vapor deposition was used in order to get a triangle with a vertex pointing upwards. The idea was to deposit metal balls or arcs on the edges of rectangular micro heat pipes to get a triangular geometry between the two adjacent metal blobs as shown in fig. 2.3. The processes used before the Cu depositions were a lot common to other works from growth of oxidation to etching the grooves. Molybdenum crucibles were machined in order to hold Cu while vapor deposition. To completely close the grooves, dual vapor deposition followed by dual vapor deposition using planetary substrates was used [10]. The adhesion of a copper layer with the wafer was improved by depositing 500 Å<sup>0</sup> of chromium and 1250 Å<sup>0</sup> of gold. Chromium adhered excellently to

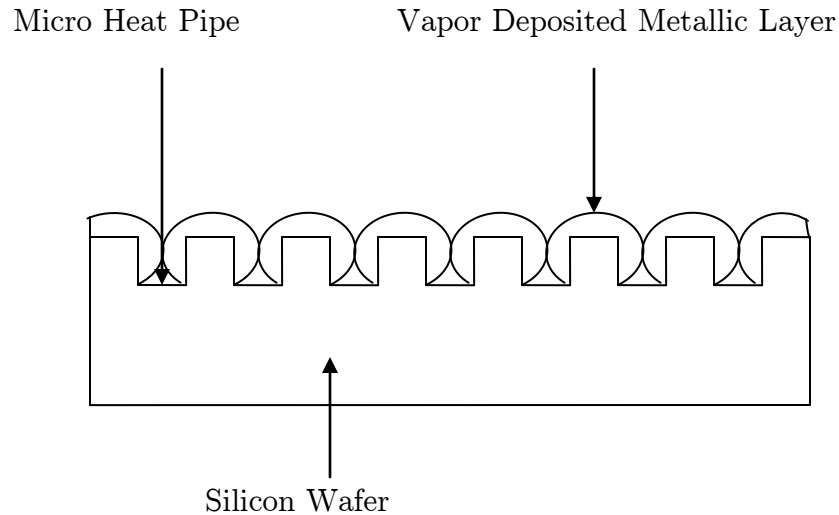


**Figure 2.3:** Proposed vapor deposited micro heat pipes by Mallik et al.[10]

the silicon, while gold compensated for the large thermal coefficient of expansion difference between chromium and copper [10].

Three types of wafers were fabricated. The first one had 34 rectangular grooves which were  $27.1\ \mu\text{m}$  deep and  $25\ \mu\text{m}$  wide. The actual coated thickness was equal to  $38.65\ \mu\text{m}$ . The second wafer also had 34 grooves which were  $24.1\ \mu\text{m}$  deep and  $25\ \mu\text{m}$  wide. The total thickness of deposited vapor was predicted to be  $31.45\ \mu\text{m}$ . The third one had 66 grooves,  $25\ \mu\text{m}$  wide and  $22.97\ \mu\text{m}$  deep. The predicted thickness of vapor deposition coating was  $48.79\ \mu\text{m}$ . The micro heat pipe arrays were covered with glass using Norland Optical ultra-violet sensitive adhesive as a bonding material.

The charging of micro heat pipes was carried out in a different way. The heat pipe arrays were kept vertical with the open ends facing downwards in a vacuum chamber. The chamber was evacuated before filling the charge. After evacuation a determined amount of methanol was let in to the chamber using a micro syringe. The initial methanol evaporated, but as the pressure inside the chamber increased and approached the saturation pressure of ethanol, additional methanol formed a pool of liquid. Once the trough was filled with enough liquid to touch the open ends of the micro heat pipes, the liquid was wicked up in the pipes due to capillary forces. After filling the array, the micro heat pipes were removed from the vacuum chamber and effectively sealed with a low vapor epoxy.

Y.X. Wang and G.P. Peterson [11] tried to construct a micro heat pipe array in quite a different way. The concept was to bond several arrays of wires between two metal plates so that the gap between them will act as a micro heat pipe array. The concept is shown in fig. 2.4. The sharp edges between the metals and wires would act as an artery [11]. The plates taken were 152.4 mm by 152.4 mm in dimension. The heat pipe was conceptually divided in three areas: an evaporator section of 25.4 mm, an adiabatic section of 93 mm. And a condenser section of 34 mm.

There were six micro heat pipe arrays tested. The wire diameters and wire spacing were used in the study. While testing, two electrical resistance film heaters were used to generate heat. The temperature distribution on the surface of the micro heat pipe array was measured by 24 thermocouples. The condenser was placed between two cold plates and the operating temperatures were maintained between 20°C to 50°C. The results showed that the heat carrying capacity of the micro heat pipes increased with the operating temperature. There was an optimum operating temperature at which maximum heat transport capacity was attained.



Further, it was observed that this optimum temperature increased with the wire diameter. For an example, the optimum operating temperature was 50°C when wire diameter was 0.33 mm and 70°C when the wire diameter was 0.635mm. The wire spacing also played an important role in heat carrying capacity. The increased spacing was observed to be helping a single micro heat pipe but was reducing the heat carrying capacity of an array since the increased spacing resulted in smaller number of micro heat pipes in an array.

Polymer micro heat pipes were fabricated by Wai Y. Liu et al [12] for InP/InGaAs technology. They eliminated the high temperature wafer-to-wafer bonding process. The heat pipe was conical in shape with the evaporator at the tapered end

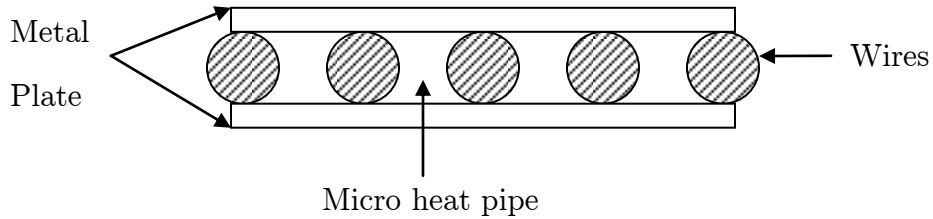


**Figure 2.4:** Micro heat pipe array tested by Wang et al. [11]

and condenser at the other. The conical shape allowed reduction in vapor flow which relaxed the entrainment limit [12].

The heat pipes were fabricated in photo-curable resin. 2.5mm of resin was put on a substrate and guarding rings, at the edge of the conical structure were created on the resin using a proper photomask. A metal ball was then placed at the position where the micro heat pipe was desired and pushed into the resin. The wafer was then cooled to room temperature. The final geometry was achieved by selectively exposing the resin to a UV radiation source. A mixture of metal powders and thermally curable resins were used to form the wick. The mixture was prebaked, and then stirred to get cracks and pores in the resin. The mixture was then applied to the area where the wick was desired. In the test setup, the on chip resistor served as the heater and the thick metal plate attached at the bottom served as heat sink. The micro heat pipe was sealed with a metallic lid. The radius of evaporator was 0.5mm and that of condenser was 2.5mm.

Shung-Wen Kang et al [13] fabricated and tested radial grooved micro heat pipes. It was a three layer structure: the top was vapor, the bottom was liquid phase and the middle was a separation layer, which separated the liquid and vapor flows to reduce entrainment limits created by the shear forces at the interface [13].

Three masks (one for each layer) were used to fabricate the structure. There were 70 equally spaced, trapezoidal vapor phase grooves, 23 mm in length. The outer end was 700  $\mu\text{m}$  and the inner end was 350  $\mu\text{m}$ . The liquid phase mask was same except it was 150  $\mu\text{m}$  at the inner end and 500  $\mu\text{m}$  at the outer ends. The central mask was octagonal in shape, and had a through hole of square cross-section to connect the liquid and vapor phases. There were also through grooves on the sides of octagon to connect the two phases from the condenser side. This was there as a separation formed between the vapor and liquid phases. Fabrication was done in typical steps. The central mask was double-side polished and was etched from both sides. Au-Si eutectic bonding was used to bond. Alignment was achieved

with the help of a fiber optic alignment technique. The charge was filled by evacuation technique. The amount of charge filled was controlled to 30%, 35% and 70%. An 11 mm x 11 mm silicon rubber acted as a heater in the central part of the device. Ten K-type thermocouples were used on the bottom side of the MHP, eight on the circumference and two in the middle. Five K-type thermocouples were used on the top side, four on circumference and one in the middle. The thermocouples were spaced equally. A Cu heat exchanger was used for cooling. The evaporator temperature was recorded. At 27 watts of power, the 70% filled MHP recorded an evaporator temperature of 67°C, which was 27% lower than that recorded for plain wafer. The authors also recorded the temperature difference between evaporator and condenser section. The 70 % filled gave a 33% lower difference than the plain wafer.

In one of the earlier works, G.P.Peterson et al. [14] tried to fabricate and test micro heat pipes. They fabricated two sets of micro heat pipes on silicon wafer and tested them. Then the results were tested against that observed by testing a plain (ungrooved) silicon wafer. The first set had 39 channels, which were 19.7 mm long with a width of 45  $\mu\text{m}$  and depth of 80  $\mu\text{m}$ . The channels were placed 500  $\mu\text{m}$  apart, and the wafer was 0.378  $\mu\text{m}$  thick. The first set was fabricated using a dicing saw. The geometry of the cannels was rectangular in shape. The second set had triangular channels which were fabricated with the help of an anisotropic etching process. The channels were 120  $\mu\text{m}$  wide and 80  $\mu\text{m}$  deep. Normal processes from photoresist application to etching were used. After the fabrication, a 25  $\mu\text{m}$  Pyrex cover slip was bonded to the wafers. An ultraviolet bonding procedure was used to bond both the structures. For charging the wafer, the wafer was put vertically in a vacuum chamber. One end of the micro heat pipes was sealed while the other was kept open. The open end was kept in a trough facing down. After

evacuation, the working fluid was injected in the chamber. As the chamber temperature increased and reached the saturation pressure corresponding to the chamber temperature, the fluid started to form a pool on the trough. The fluid in the pool was wicked up in the channel, sealing off the channel and trapping the vapor in upper portion of the micro heat pipe [14].

For experimental purposes, heat was generated using a thermo foil heater attached on the back surface of the array. A copper heat sink was attached on the condenser end. The temperatures were measured by an infrared thermal imaging system. Throughout the tests, the IR camera captured both wafers simultaneously, to compare the effectiveness of the micro heat pipe array. Results from the tests at 4 W powers showed that the wafer with rectangular channels had a maximum temperature reduction of 11.4°C, 31 % increase in thermal conductivity over the plain wafer readings. The triangular channels had a maximum temperature reduction of 16.2°C and thermal conductivity increased by approximately 81 % over the plain wafer readings. It was also concluded that the transient thermal response of the wafer increased significantly by the incorporation of the micro heat pipe array.

Mantelli et al. [15] tried to work out a wire plate micro heat pipe. The concept was the same as Y.X.Wang [11]. Wires were put between two flat plates. A diffusion welding fabrication process was used to fabricate these flat plate micro heat pipes. The sharp angle between wire and plate was welded without blocking the channel, and worked as a porous medium. The fabricated MHP array had overall dimensions (plate dimensions) of 78mm X 10mm with a distance between the plates of 2.05mm. The wire diameter was 1.45mm and the wires were placed at a distance of 1.45mm from each other. Heat was produced by a resistance heater. Heat was carried out from a condenser with the help of a cooling bath. Six T-type

thermocouples measured the wall temperatures. The authors observed that the thermal conductivity of a filled micro heat pipe array increased by a factor of 1.3 than observed for empty micro heat pipe array.

Shung-Wen Kang and Derlin Huang fabricated and tested star grooves and rhombus grooves micro heat pipes [16]. The micro heat pipes were fabricated by standard photolithography processes. Three <100> silicon wafers were used for star grooves micro heat pipes and two <100> silicon wafers were used for rhombus shaped micro heat pipes. Both had an array of 31 parallel grooves. After the fabrication of the grooves, the wafers were assembled with eutectic bonding, for which, the wafers were coated with 75 Å of chrome and 2000 Å of gold. The wafers were then exposed to air and heated for 30 minutes in vacuum at 500°C. The pressure used was about 1.45 Pa. The micro heat pipes were charged in an evacuated environment with the charging hole facing down. A 6 mm X 25.4 mm resistance heater was used to generate heat [16]. The heater assembly was insulated with the help of styrofoam insulation [16]. The condenser was attached to a copper heat sink which was cooled by a constant temperature fluid bath. K-type thermocouples were used to measure the temperature across the surface. The authors observed that star grooves with 60 % methanol got a reduction in maximum wafer temperature of 32°C and increased the average effective thermal conductivity by 70 % over a range of 20W. Rhombus grooves filled with 80 % methanol, gave a reduction in maximum temperature of 18°C and the average effective thermal conductivity was increased by 80 % [16].

W.Kinzy Jones et al .[17]tested a micro heat pipe fabricated in Low Temperature Cofire Ceramic (LTCC). Thermal vias were drilled in the system using a micro-drilling/micro routing system, and the system was laminated by a laminator. Prior to lamination Ag was inked in with the help of vacuum and a

porous wick was created. Silver was used for the wick structure. The micro heat pipe was charged in vacuum.

Two proto type heat pipes were fabricated. One was a rectangular single channel heat pipe, and the other was a square shaped multi channel heat spreader. Heat was generated by a thick film heater. The condenser was cooled with the help of a finned copper heat sink. The heat spreader prototype was cooled directly by forced air or impingement water cooling. Thermocouples were soldered to measure the temperature. They observed that at 16.7 W the heat spreaders highest temperature was 35°C less than that of a solid sample.

In 1991 D. Wu et al. [18] conducted an experimental investigation on small specially designed micro heat pipes. The goal was to verify operation, performance limits and transient behaviors, and a earlier developed numerical model [18]. The micro heat pipes had a tapered geometry: the bigger side was 2 mm and the smaller side was 1.3 mm. The height of the trapezoidal cross section was 0.6 mm. The length of the micro heat pipe was 60 mm. The heat pipes were charged with 0.032 g of ultrapure deionized water. The test was carried out in a vacuum chamber. Heat was generated with the help of a thin nichrome strip. The condenser was cooled with the help of a cooling chamber maintained by circulating ethyl-glycol solution. The temperature was measured with the help of eight constantan thermocouples along the length of the micro heat pipe. An empty micro heat pipe was also tested to be as a base line model. The experimental results were in agreement with numerical model for the maximum steady state transport capacity prior to dryout, the steady state temperature distribution along the longitudinal position and the steady state temperature difference between axial locations prior to the dryout.

In 2004 Gillot et al. [19] fabricated a flat silicon heat pipe with micro capillary grooves. The heat pipes were tested as heat spreaders. Three wafers were used to fabricate the heat pipes. The wafers were 100mm in diameter and 500  $\mu\text{m}$  in thickness. Top and bottom wafers had grooves with width of 90  $\mu\text{m}$  and depth of 115  $\mu\text{m}$ . The grooves were fabricated using deep plasma etching technique. Small holes were laser drilled on the top wafer for filling purposes. The wafers are bonded with the help of hydrogen molecules between the wafers and Van der Waals forces. The metallization layer was sputtered around the laser drilled hole to solder copper tube for filling purpose. For testing purposes, a copper heater was deposited on the silicon substrate. The heat pipe was glued to copperplate which was cooled with water. Infra thermal imaging was used to measure the temperatures. The tests showed that the filled micro heat pipes reduced the thermal resistance to 0.8 K/W from 2.3 K/W, which was observed in the empty micro heat pipe.

Rengasamy ponnappan [20] fabricated and tested a novel screen wick design suitable for a miniature heat pipe. The idea was to provide a simple and low cost fabrication of micro wick structures [20]. The wick was made of commercially available wick cloth. A wavy corrugated pattern was formed on the screen with the help of a fin making process. The pattern was rectangular 0.2 mm wide and 0.9 mm deep. The screen was then enveloped and fitted in a rectangular copper tube. End caps were fitted and the tube was filled with charge by a fill tube from one of the sides. For the experimental setup, a total of nineteen T-type thermocouples were used. Eight were on the top, eight on the bottom and three on the sides. Six thick film resistors were used to simulate heat sources and the condenser section was cooled by two coolers clamped on it. It was observed from the tests that heat flux of 115  $\text{W}/\text{cm}^2$  at an operating temperature of 90°C was reached, and the evaporator to adiabatic temperature difference was 37°C.

Hallinan et al. [21] tested micro heat pipes to show electro-hydrodynamic augmentation of heat transport in micro heat pipe arrays. The micro heat pipe array was fabricated from quartz flat. The channels were 1 mm wide and 0.9 mm deep. Gold-palladium electrodes were deposited on both sides of micro heat pipe arrays to attain an electrostatic field of 10 kV/mm. During the experiment, the heat input was given through resistance heating element. And heat was rejected through the cold jackets attached at the condenser end of the device. Five 36 gauge thermocouples were attached on the ground side with the help of thermally conducting epoxy. A cover slide was used to cover the micro heat pipe arrays. The results showed that the electric field slowed down the evaporator dryout [21]. It was also seen that with the electric field, the heat transport roughly double that of ,with no electric field, was observed before the micro heat pipe failed due to thermal stresses induced in the glass in the proximity to the heater [21].

Laura J. Meyer et al. [22] fabricated a silicon-carbide micro capillary pumped loop. In a capillary pumped loop, the evaporator and condenser sections are connected by separate liquid and vapor lines. The loop was fabricated from silicon carbide wafer and glass. The condenser wick structure was formed in glass. Glass was used to do visual inspection of the operation. The evaporator, condenser and connecting lines were fabricated in silicon carbide with a depth of 150 microns with vertical side walls. The capillary wicking structure was 30 microns deep and 6-30 microns wide with trapezoidal sidewalls [22]. The capillary grooves were dry etched to get sharper edges. Glass and silicon carbide wafers were bonded with the help of an adhesive film.

It was observed from the literature review that the fabrication processes used for silicon based micro heat pipes were similar in most of the works. Water and methanol were used as working fluids by many of them. One of the works,



which was reviewed, discussed on the possibility of using liquid metals as working fluids in micro heat pipes [6]. The authors built a prototype using water as a working fluid and also formulated a numerical model to estimate specific conductivity of micro heat pipes using liquid metals.

In the work discussed in this thesis, micro heat pipes were fabricated using similar fabrication processes as the earlier works. Mercury was filled in and the pipes were sealed using indium cold welding. Tests carried out were aimed to check the feasibility of using mercury as a working fluid.

## CHAPTER 3

### FABRICATION OF MICROHEAT PIPES

#### 3.1 Introduction

This chapter deals with fabrication techniques for the micro heat pipes. The micro heat pipes were made by assembling two rectangular 5 x 10 mm dies. One containing the channels and the other consisting the lids with sensors and a groove to put heating element into it. The tests and results of the micro heat pipes are discussed in next chapter.

#### 3.2 Design and dimensions of the micro heat pipes

The micro heat pipes were fabricated from two separate wafers, one on which channels were etched and another used to fabricate lids for the channels. After the fabrication, the dies with channels and lids were bonded together by Indium cold weld processes.

The channels were square in cross section, 100 microns wide, 100 microns deep and 9500 microns in length. There were 22 channels in each die with a 100 micron pitch and the wafer was designed to yield 44 such dies. For the fabrication of the channels the wafers used were single side polished. The orientation of the

wafer was 100 or 110. The thickness of the wafers was 300 microns and the wafers used were 4 inch in diameter.

The lids were fabricated such that the underside had a pattern similar to the channels so they would mesh with the channels while bonding. The pattern was etched 20 microns deep to accommodate the metallic layers. The top of the lid had 5 platinum sensors patterned on it. These sensors were in a serpentine form, each patterned onto an 800 micron by 1000 micron area. The sensors were either 26560 microns or 26980 microns long and were 10 microns wide.

A groove was also etched on the top side of the lid to allow for a heating wire. The groove was 250 microns deep, 1000 microns wide and 5 mm long, 1 mm away from the edge of the die.

### **3.3 Fabrication of channels**

The micro heat pipes were fabricated in the Alabama Micro Science and Technology Center (AMSTC), in a class 100 clean room. The fabrication of the pipes requires a silicon wafer to go through a number of processes. The processes were carried out in a controlled environment and required precise supervision to get a suitable end product; the cleanliness, in particular is critical in the resulting product.

#### **3.3.1 Cleaning of the wafer**

The wafers were cleaned using SEMITOOl's spin rinse dryer. The machine rinsed the wafers in de-ionized water as they spun and then spun dry them. The wafers were cleaned to remove any surface impurities. These impurities if not removed, could disturb the pattern in later stages of the fabrication process.

### 3.3.2 Dehydration bake and Hexamethyldisilazane (HMDS)

The wafers were then put in an IMPERIAL IV microprocessor oven for the dehydration bake. They were inside the oven for 20 minutes at 120°C, to remove any moisture from the wafers' surface, which improves the photoresist bonding on the wafer. A dehydration bake is required when ever the wafers are exposed to the atmosphere for a long period of time before putting on the photoresist.

After the dehydration bake, the wafers were kept in hexamethyldisilazane (HMDS) chamber for 20 minutes. HMDS is coated over each wafer to chemically dry the wafer and improve the photoresist adhesion.

### 3.3.3 Photoresist application

A photoresist is a substance which is applied to a wafer so that a pattern can be created on it. It is a photosensitive material which will not be removed by exposure to acid or developer. Application of the photoresist is an important step in the fabrication process. There are two types of photoresist: positive and negative. A positive photoresist has a higher developer dissolution rate when exposed to light. A negative photoresist, on the other hand becomes relatively insoluble to developer when exposed to light. A positive photoresist is used when the transparent parts on the mask are to be patterned on the wafer; a negative photoresist is used when the opaque parts on the mask are to be patterned.

There were two types of photoresists used to pattern the channel mask onto the wafer. Initially a negative photoresist was used to block the channels and expose the walls of the channels in the pattern. This helped deposit Indium on the top surface of the walls, a necessary step for the bonding of channels and the lids. The wafer was then placed in the CEE spinner. AZ<sup>R</sup> nLOF<sup>R</sup> 2035 photoresist was applied, and the spinner was operated at 3000 rpm for 30 seconds, which left 3µm

thick layer of photoresist on the wafer surface. Fig. 3.1 shows a schematic of the photoresist applied onto the wafer.

In the later stages of the fabrication, positive photoresist was used to expose the channels, to allow for etching. The photoresist used was AZ<sup>R</sup> 5214-EIR (1.3 $\mu$ m) for water-filled micro heat pipes, STR<sup>TM</sup> 1045 (5 $\mu$ m) for mercury-filled micro heat pipes. They were also used at 3000 rpm for 30 seconds.

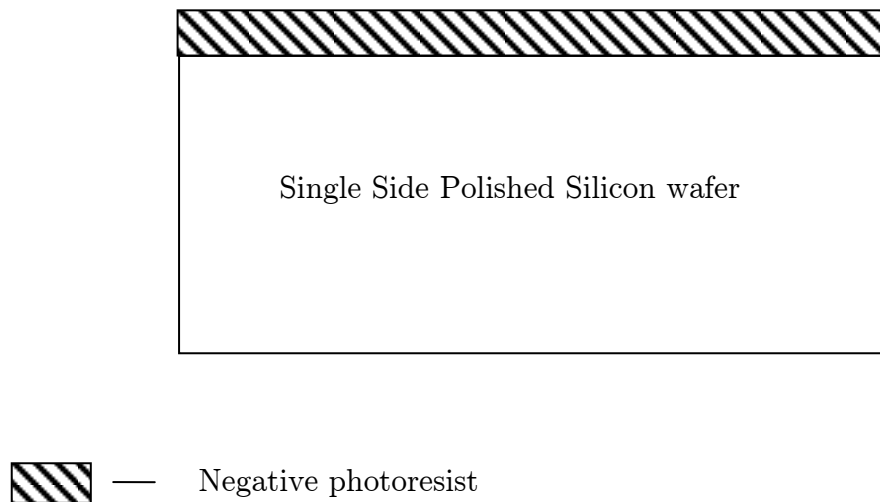


**Figure 3.1** : Wafer with negative photoresist

### 3.3.4 Soft bake and hard bake

A soft bake was performed after the photoresist was applied on the wafer. It dried the applied photoresist film and improved their adhesion. A hard bake, requiring a higher temperature than a soft bake was carried out after developing the pattern. It killed the photosensitivity of the photoresist and stabilized the photoresist in preparation for the next processes.

While using the negative photoresist the wafers were baked on a hot plate at 90°C for 1 minute after applying the photoresist. After exposing the pattern the wafers were again baked at 90°C for another minute.

### 3.3.5 Mask Alignment and Developing

A mask is a glass plate with both opaque and transparent patterns on it, used to create the desired pattern on the wafer. The mask must be carefully aligned with the wafer to create the desired pattern. The mask has alignment marks in case we have to use more than one mask for a pattern. Alignment of the mask and exposing is done on the mask aligner, a device which transfers the pattern from the mask to the wafer with the use of photolithography and exposure. Usually an aligner is also equipped with UV light to perform the exposure. An aligner is of particular importance when creating multilayer patterns.

The mask we used is shown in fig. 3.2. Fig. 3.3 shows a zoomed image of one of the die patterns with 22 channels on it. The pattern from the mask was transferred to the wafer with the help of KARLSUS MA6/BA6 mask aligner. After the alignment the UV light was active (exposure time) for 12 seconds. Since a negative photoresist was used, the exposure was followed by baking on a hot plate for 1 minute at 90°C.

After alignment and exposure, the image was developed in the developing room. Developing is the process where by the developer interacts with the

photoresist to resolve an image. There are different developers for negative and positive photoresists. The main difference is in their attack rates. A positive photoresist developer has a high attack rate on the exposed part compared to the unexposed part of the photoresist, and the negative photoresist developer has higher rate on the unexposed part of the photoresist.

AZ<sup>R</sup> 300 mF developer was used with no dilution for developing the pattern. This developer was used since a negative photoresist was used. In the developing room, the developer was placed in a tray and the wafers were put in it for 2 minutes and 15 seconds. The developing process was followed by thoroughly cleaning the wafers with de-ionized water and drying them with nitrogen. The wafers were checked under the TERRA UNIVERSAL inc. microscope to make sure the patterns were as desired.

Later the wafers were put in a flood-exposing unit for 5 seconds, to tighten the pattern. Flood-exposing was followed by hard bake at 110<sup>0</sup>C for couple of minutes. Fig. 3.4 and 3.5 show the schematic diagrams of the photomask exposure and the developing of the photoresist.

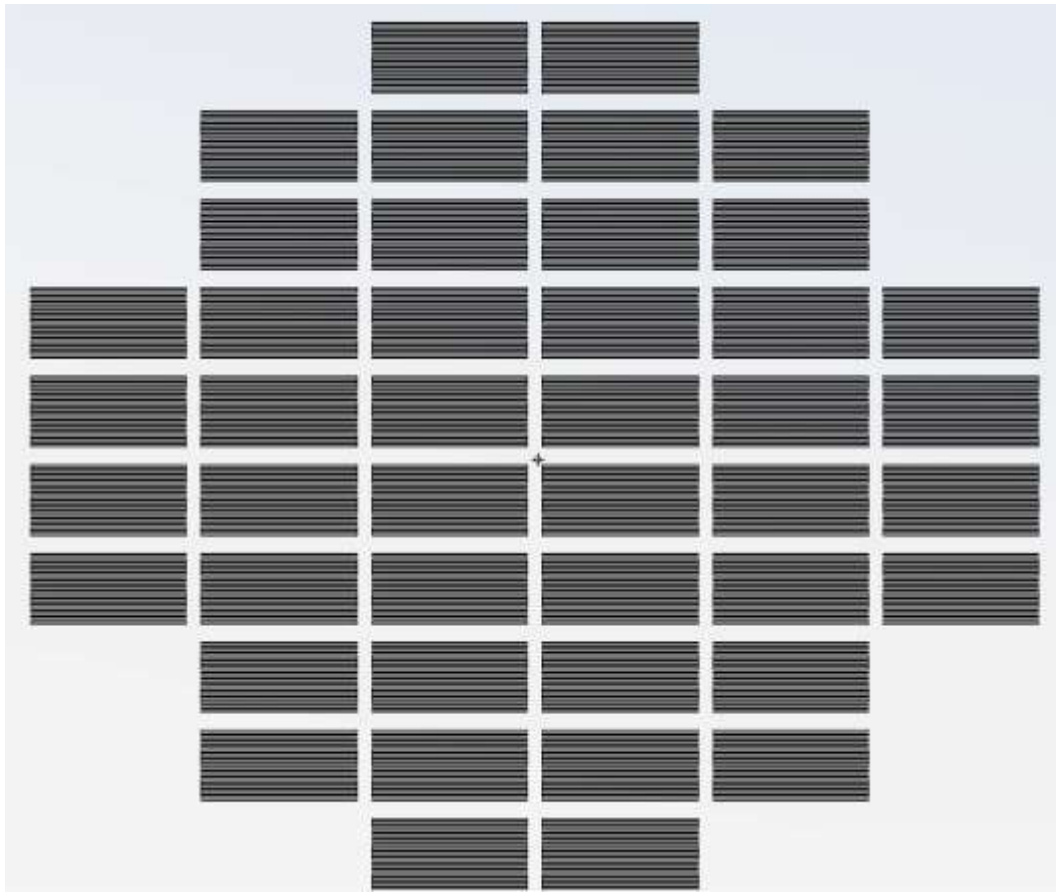



**Figure 3.2** : Channel's mask (44 dies)



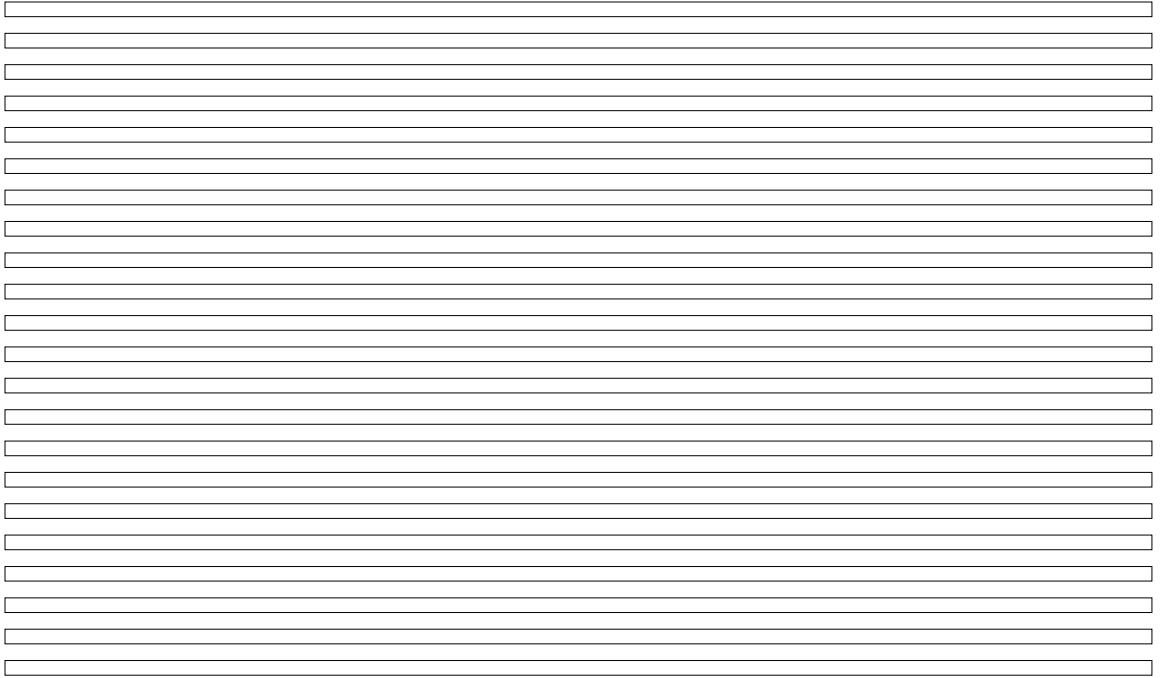
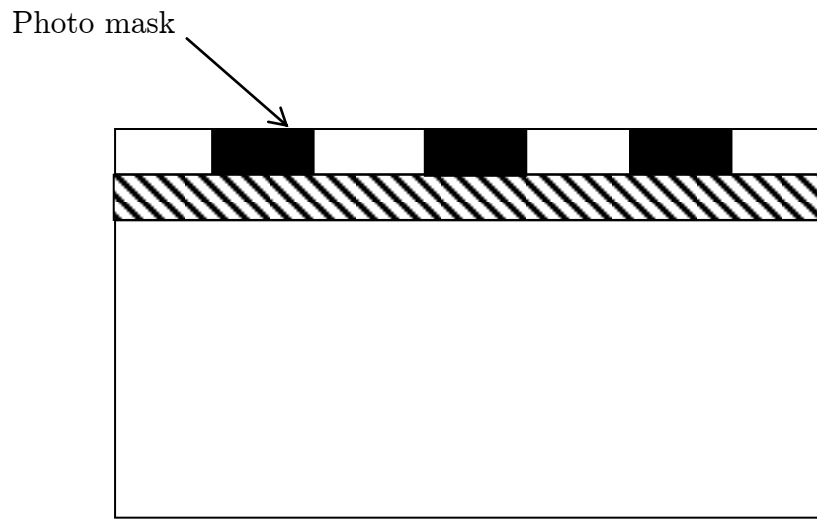
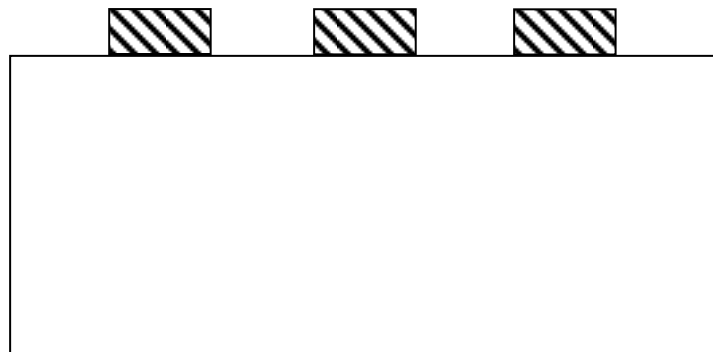



**Figure 3.3** : Single Die (22 channels; 100 microns x 9500 microns)



 — Negative photoresist

**Figure 3.4** : Alignment of mask.



 — Negative photoresist

**Figure 3.5** : Developed photoresist

### 3.3.6 E-beam deposition and Ultrasonic strip off

An e-beam evaporator is a machine where layers of different metals are deposited on the wafers. In the e-beam evaporator, a high intensity beam of electron strikes the target and melts a region of it. The material then evaporates to cover the silicon wafer [23]. We used CHA INDUSTRIE's mark 50 e-beam evaporator.

Layers of titanium, nickel and indium were deposited on the wafers with the e-beam evaporator at thicknesses of  $500 \text{ \AA}$ ,  $300 \text{ \AA}$  and  $10,000 \text{ \AA}$  respectively.

Indium is used for bonding but since it does not adhere to silicon very well, it had to be deposited on a thin layer of nickel. And for nickel to adhere to silicon, a layer of titanium was used. Figure 3.6 shows the position of a Ti/Ni/In layer on a wafer.

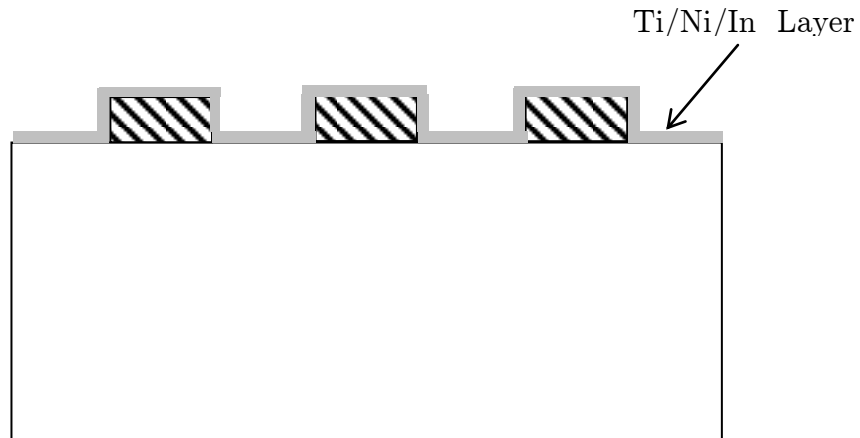


**Figure 3.6 :** Position of Ti/Ni/In layer.

### 3.3.7 Ultrasonic photoresist strip off

After the Ti/Ni/In layers were in place, the photoresist was removed using an ultrasonic photoresist strip off.

The wafers were put into a glass vessel containing acetone and the vessel was put into an ultrasonic cleaner. The time required for the photoresist to come off varies so the vessel was kept under constant observation and removed when the photoresist was completely stripped off.

This left the deposited indium on the walls of the channel and removed it from every where else. Figure 3.7 shows the surface after the ultrasonic strip off.

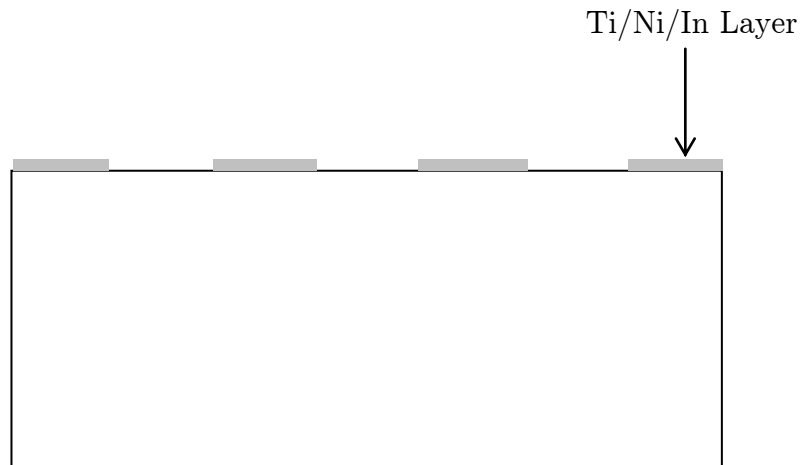


**Figure 3.7** : Surface after the ultrasonic strip off

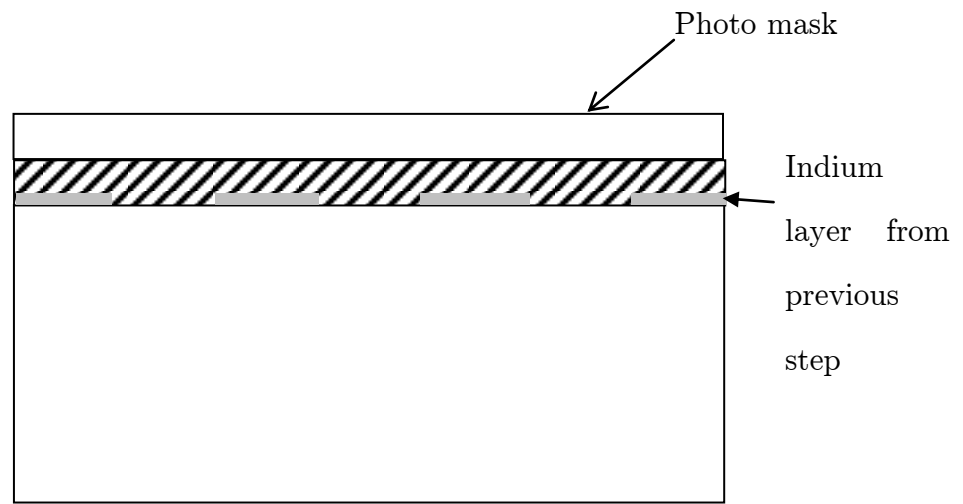
### 3.3.8 Repeat procedure from Dehydration bake to Developing


After the photoresist strip off processes, the procedures from dehydration bake to developing were repeated. This was done to cover the indium on the walls of the channels with photoresist so the wafer could be introduced in the etcher.

This time the photoresist used was STR<sup>TM</sup>1045 for the mercury micro heat pipes and AZ<sup>R</sup>5214-EIR for the water micro heat pipes. STR<sup>TM</sup>1045 forms a more thick and viscous layer and, hence, was used in mercury micro heat pipes since they required a complete and clean photoresist removal on the preceding procedures. The above mentioned photoresist can also be used for water filled micro heat pipes.

After the application of the photoresist, we performed a 2 minute soft bake for STR<sup>TM</sup>1045 and 105<sup>0</sup>C for AZR5214-EIR

The mask was aligned properly so the opaque portion aligned with the channel walls pattern and the transparent portion aligned with the channels pattern on the wafers. The exposure time was 30 seconds for STR<sup>TM</sup>1045 and 8 seconds for AZ<sup>R</sup>5214-EIR. Developing was done in AZ<sup>R</sup> 400 K developers. The developer was mixed in 1:3 ratios with water and the wafers were kept in the solution for 2 minutes and 15 seconds. The flood exposure and hard bake procedures were then repeated as earlier. Application of the positive photoresist is shown in figure 3.8.



 — Positive Photoresist

**Figure 3.8 :** Application of the positive photoresist

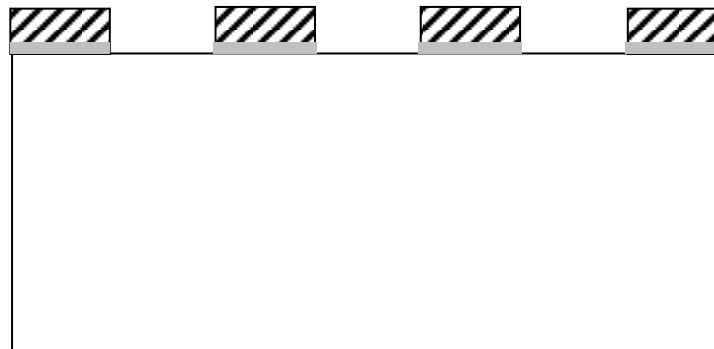


**Figure 3.9 :** Wafer after developing

### 3.3.9 Etching

Etching is the process of removing material with the help of chemical reactions. We used DRIE (deep reactive ion etching) to form the channels with vertical walls. Etching was carried out in SURFACE TECHNOLOGY SYSTEM's (STS) advanced silicon etcher. The wafers were put in for 33 minutes and 20 seconds, enough time for 100 cycles. Each cycle etches 1 micron in depth, so the 100 cycles resulted in channels 100 microns deep. The depth was checked on the profile meter or under the micro scope. Figure 3.10 shows a schematic of an etched wafer.

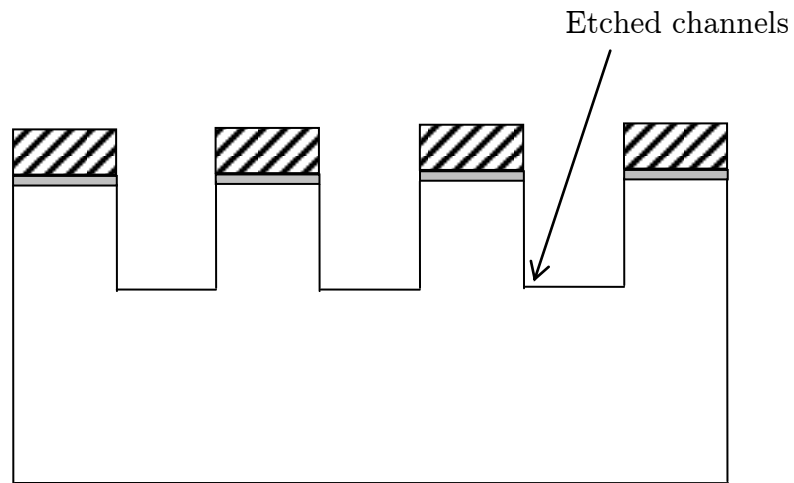


**Figure 3.10** : etched wafer

### 3.3.10 Deposition of Ti/Pt/Au and Photoresist Removal

The wafers were then put in the e-beam evaporator machine for the deposition of titanium, platinum and gold at thickness of  $100 \text{ \AA}$ ,  $1000 \text{ \AA}$  and  $150 \text{ \AA}$  respectively. The titanium was used to support the platinum. And the gold was used as a sacrificial layer: mercury consumes the gold layer and then wets platinum in its purest form [24]. Fig. 3.11 shows an experiment carried out where a drop of mercury was put on test wafer coated with Ti/Pt/Au.





**Figure 3.11** : Mercury on a Ti/Pt/Au wafer

After the deposition of the metal layers, the wafers went through the photoresist strip off processes. The wafers were then cleaned using de-ionized water and nitrogen and were ready for dicing. Figs 3.12 and 3.13 show the deposition of the Ti/Pt/Au layer and a wafer after the photoresist strip off.

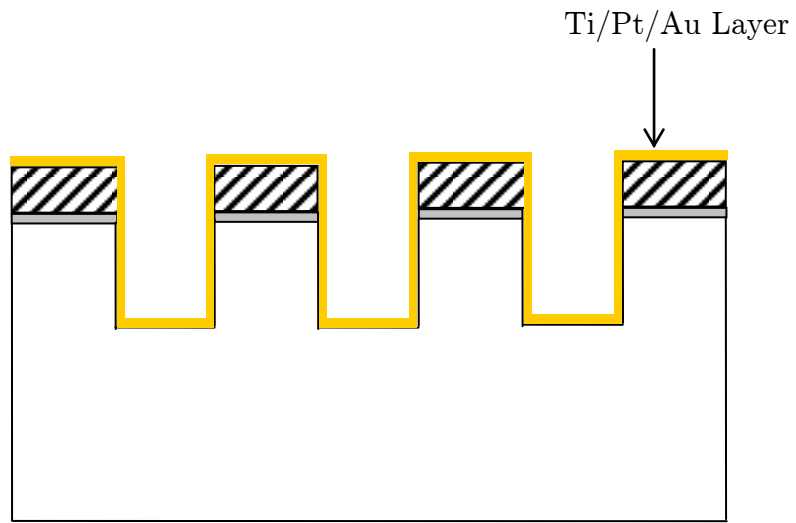


**Figure 3.12** : Wafer after Ti/Pt/Au deposition

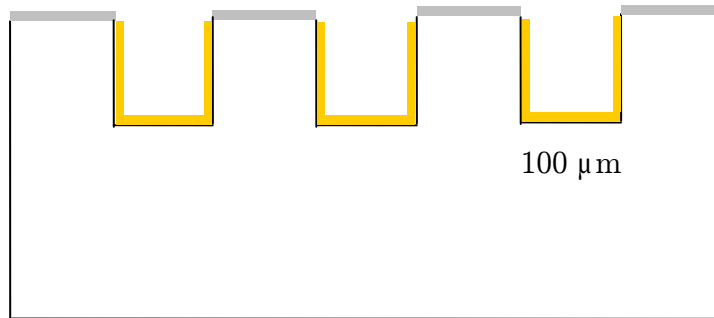


**Figure 3.13** : Channel wafer after all the procedures.

### **3.3.11 Dicing**

The next step was cutting the wafers and separating the dies. The motions of a dicing saw are electronically controlled. The dicing saw needs to be programmed before starting the operations. The wafer needs to be attached to a plastic film before starting the dicing operation. The plastic film is supported by steel rims.

We used MICRO AUTOMATION's electronically controlled dicing saw and SEMITEK's silicon dicing blade for this operation. Though the dicing machine was programmed, we maintained visual observation during dicing to ensure that the blade was in the exact center of the two adjacent dies.

After dicing, the rim was detached from the machine. The wafers were washed with de-ionized water and dried with nitrogen. Then the whole rim was kept in the flood-exposing unit with the wafers facing down, to loosen the glue on the film which holds the wafer. This made removing the dies from the film much easier. After the flood-exposing processes the dies were detached with tweezers and kept in a Petri dish.

The whole procedure described above produced 44 dies with 22 channels in each. The bottoms of the channels were plated with Ti/Pt/Au and the top of the channel walls were plated with Ti/Ni/In.

### **3.4 Fabrication of the lids**

The lids were put on top of the channels so that rectangular pipes were formed; every die made for 22 such pipes. The lids were fabricated from double side polished silicon wafers; with a thickness of 500 microns each. They had sensors on one side and a pattern, similar to that of channels, on the other. This ensured that the indium plating on the channel walls and on the lids matched perfectly; a

critical factor in bonding. The process followed for the fabrication of the lids was similar to that of the channels with some minor variations. Hence we will look at the portions of the process which were different from those described above.

### 3.4.1 Oxidation

Oxidation is a process where an oxide layer is formed on the wafers. A  $\text{SiO}_2$  layer is formed on the wafer when oxygen or water vapors are reacted with the Si wafers at high temperature.

Oxide was deposited to form a barrier between the two sensors. The thickness of the oxide layer was 0.5 microns, after one hour of wet oxidation in the oxidation furnace. Fig. 3.14 shows a schematic diagram of a wafer with oxide deposition.

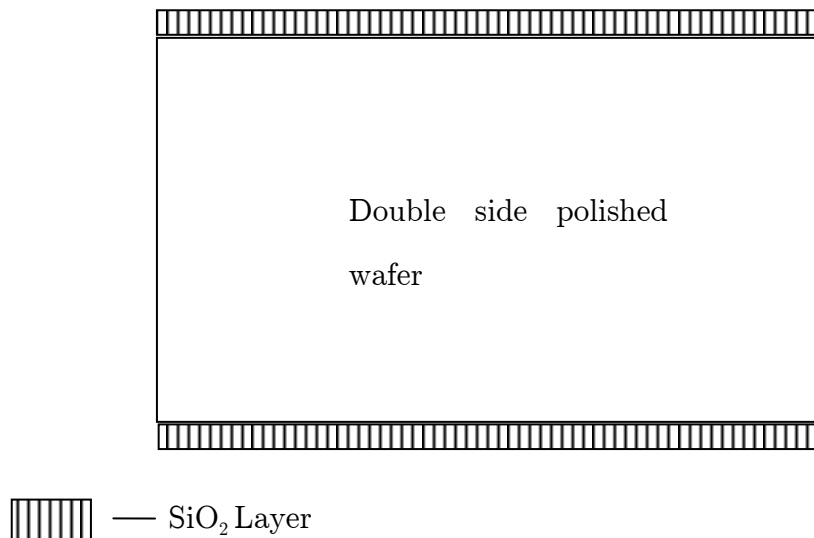


**Figure 3.14** : Double side polished wafer on both sides of the wafer

### 3.4.2 Repeating the Procedures

The procedures starting from cleaning to developing were repeated as described earlier but the photoresist used this time was AZ<sup>R</sup> 5214-EIR. We first processed the side which was going to face the channels, so the mask we used had a similar pattern as the channels. There were two masks used in this procedure to ensure that no indium was plated on the area covering the actual channels; it was only plated on the area which faced the channel walls. The first mask had the same pattern, but it was reduced by 5 microns on each side.

After exposing and developing the first mask (fig. 3.23) and after the flood exposing and the hard bake, the wafers were put in the e-beam machine for the deposition of Ti/Pt/Au for the same thicknesses as stated above. In order to save time and money, the lid wafers and channel wafers were put in the e-beam machine at the same time for the Ti/Pt/Au deposition. This procedure was followed by the photoresist strip off, allowing the Ti/Pt/Au layer to stick on the exposed part.

The photoresist strip off was followed by the dehydration bake and HMDS and this was followed by spinning the negative photoresist. The second mask was then patterned on the wafers and developed, and they then flood-exposed and hard baked. The sensor side of the wafers was then covered with the saw tape, to protect the oxide on the surface while doing the buffer oxide etch on SiO<sub>2</sub> layer. The etching solution used is a combination of HF and NH<sub>3</sub>F. HF etches SiO<sub>2</sub> while NH<sub>3</sub>F reduces the attack on photoresist by increasing the pH of the solution [25]. The wafer was kept in the solution for 5 minutes with strict visual observation. The wafers then went through the normal etching machine as described earlier, except the wafers were kept inside for 6 minutes and 40 seconds or 20 cycles giving etching 20 microns deep. This gave a design like the channels; the only difference

was that the walls on the lids were matching the channels. This ensured a perfect matching between channels and the lids.

The wafer was then put in the e-beam machine for deposition of titanium and copper at thicknesses of  $500 \text{ \AA}$  and  $10,000 \text{ \AA}$ , respectively. The Ti/Cu layer was deposited in order to plate 10 microns of indium on it. After the deposition of Ti/Cu, the wafer went through another photoresist strip off process. At the end of this process, we had wafers with dies containing channels 20 microns deep. The bottoms of the channels had a Ti/Cu layer and the walls of the channels had a Ti/Pt/Au layer.

The wafers were then sent to DCI AEROTECH, Detroit for indium plating. 10 microns of indium was plated on the side facing the channels to ensure a leak proof bonding. The whole process is explained schematically in figs. 3.15 to 3.23.

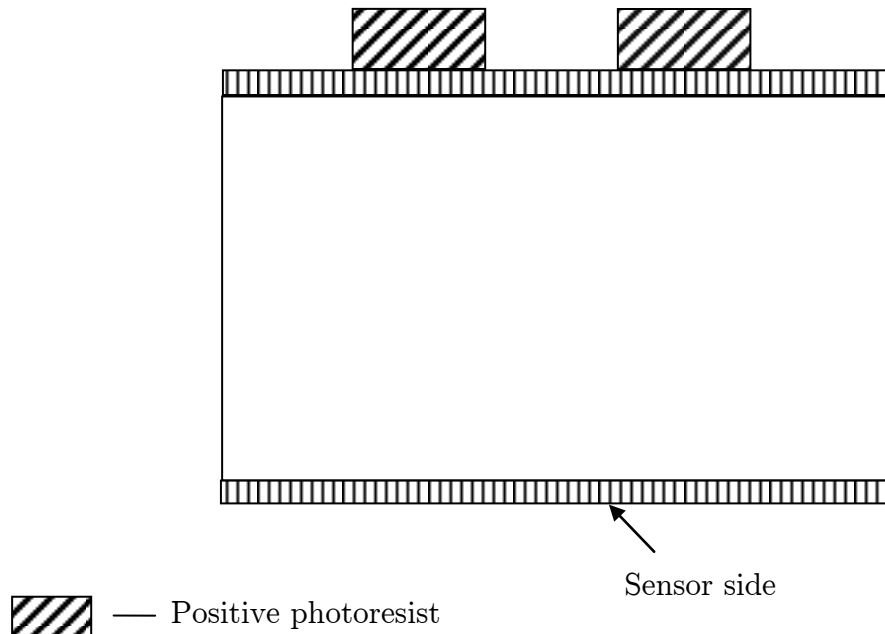


**Figure 3.15 :** Wafer after application of photoresist and exposure and developing of first mask

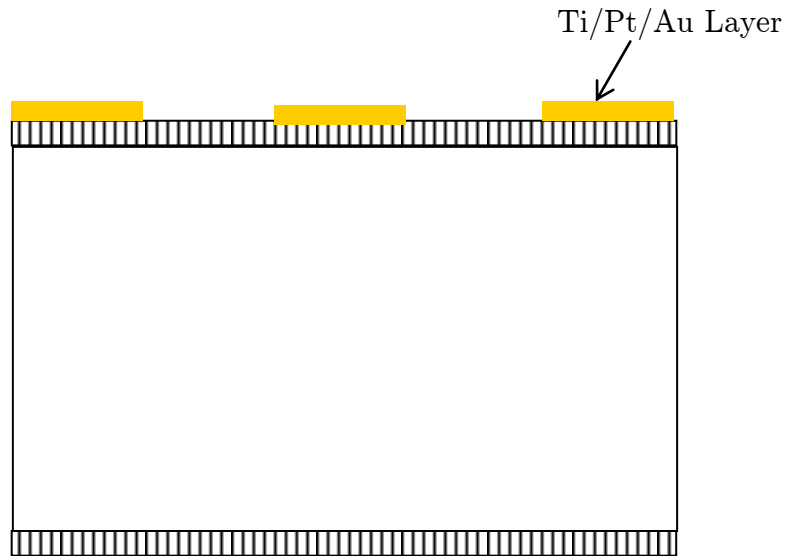
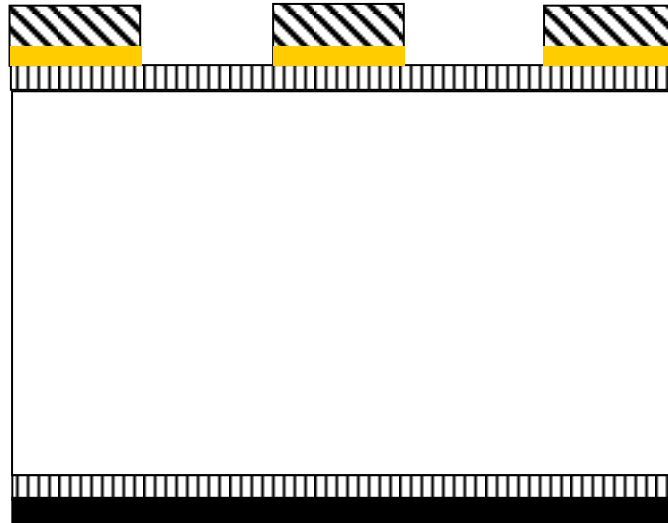



Figure 3.16 : Deposition of Ti/Pt/Au layer and photoresist strip off.



 — Negative photoresist

**Figure 3.17 :** Application of negative photoresist



 — Saw tape

**Figure 3.18 :** Wafer after exposing to mask 2 and developing. Saw tape is also put on the back side of wafer to protect that surface while buffer oxide etch processes.



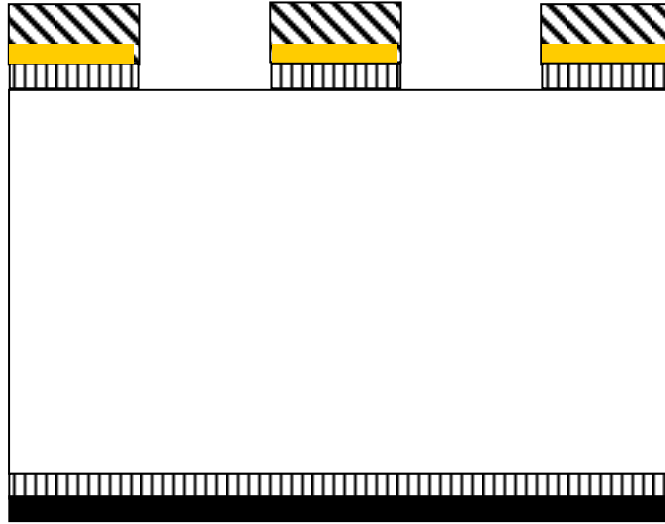


Figure 3.19 : Buffer oxide etch processes.

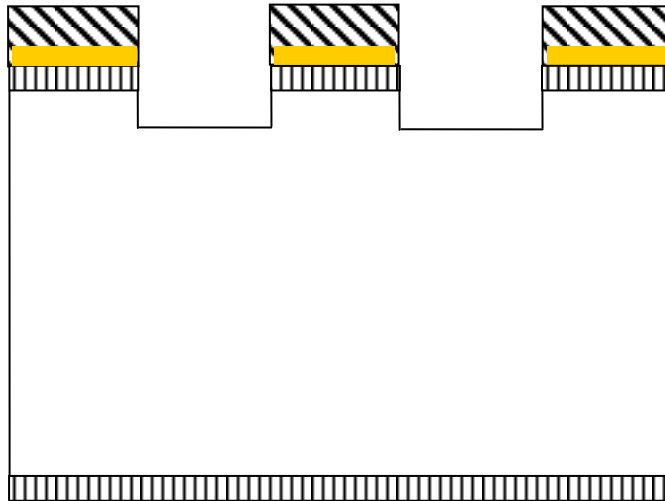
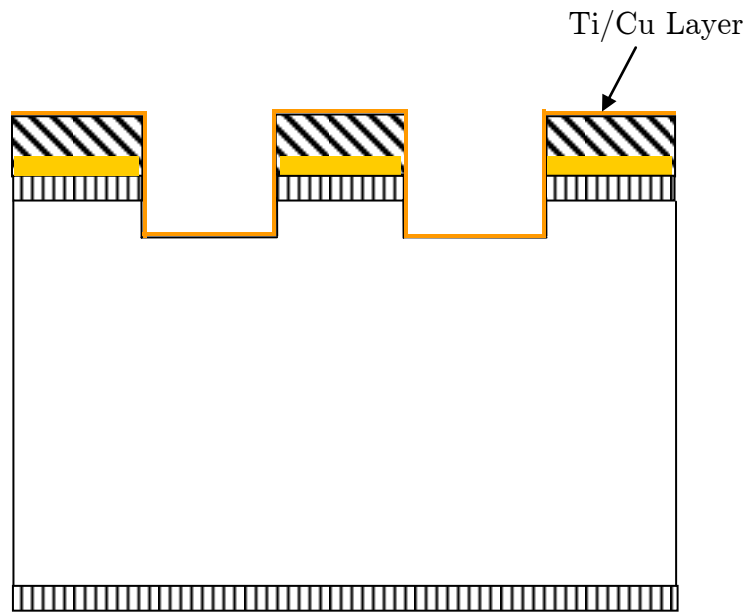
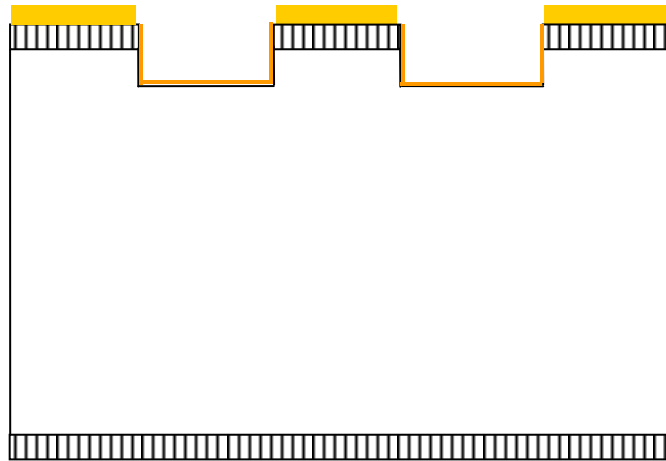


Figure 3.20 : DRIE



**Figure 3.21** : Application of Ti/Cu Layer



**Figure 3.22** : Photoresist strip off.

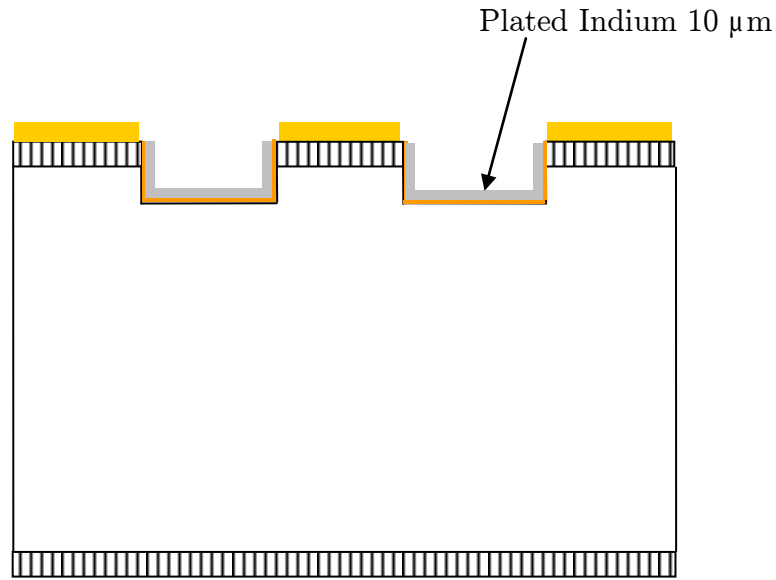


**Figure 3.23** : Indium plating (10  $\mu\text{m}$ )

### 3.4.3 Argon ion In-on-Au In ablation

In this process, Argon ions were bombarded onto the plated wafers in an e-beam machine in order to remove some traces of indium plated onto the gold coating. This process was carried out only if the indium had been plated onto the gold surface.

### 3.4.4 Fabrication of Sensors and grooves

The procedures followed for the sensors were same as described above. The wafers were cleaned and put in a dehydration bake followed by HMDS. We used the AZ<sup>R</sup> 5214-EIR photoresist, and the wafers were exposed to a sensor pattern. The wafers were then developed and put in the e-beam machine to deposit the

Ti/Pt/Au in the same thicknesses described earlier. This process was followed by the ultrasonic photoresist removal.

While exposing the wafers to the sensors mask (fig 3.26, 3.27, 3.28), we were careful to align them perfectly. It was necessary for the sensor mask to align properly with the pattern on the back side and we accomplished this with the help of back side illumination technique provided by the KARL SUSS MA6/BA6 mask aligner.

The grooves required for holding the heating wire were fabricated next. The only difference in this procedure was that a different mask for the grooves' pattern was used. After developing the pattern, the wafers were kept in SURFACE TECHNOLOGY SYSTEMS advanced silicon etcher for 83 minutes and 20 seconds or 250 cycles, creating grooves 1 mm wide and 250 microns deep. This process was followed by cleaning and dicing. At the end of this procedure, we had dies with sensors and grooves on one side and a matching pattern on the other. The final assembly is schematically shown in fig. 3.30.

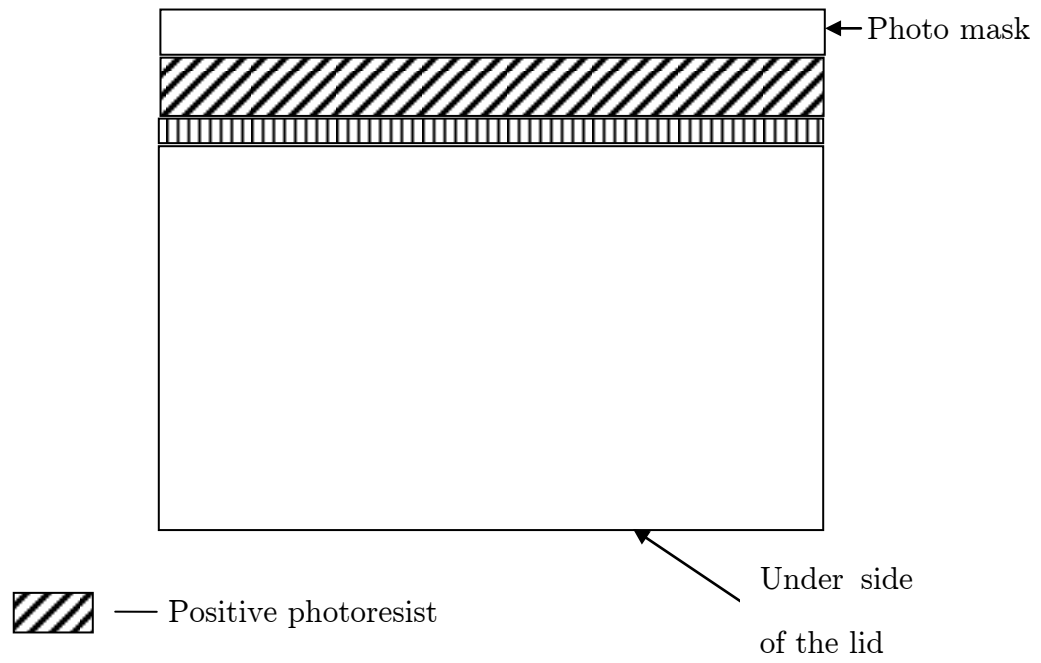


Figure 3.24 : Application of positive photoresist and exposing the sensor mask.

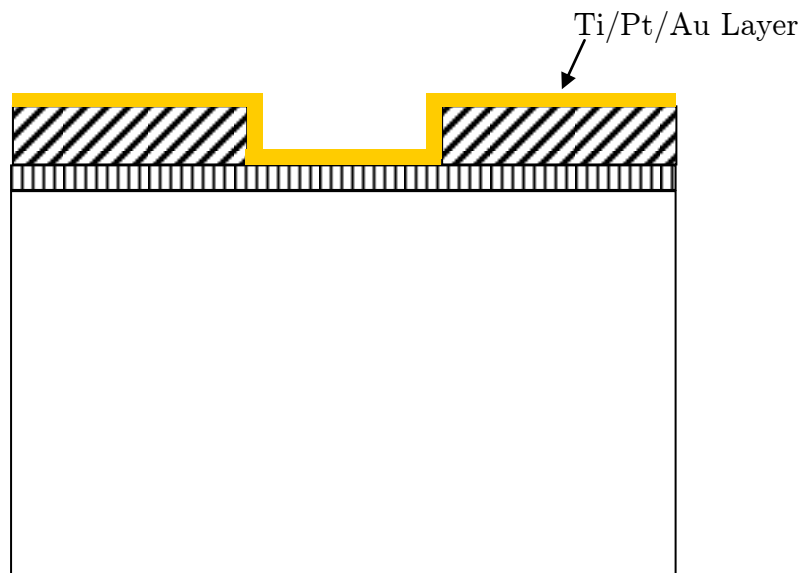
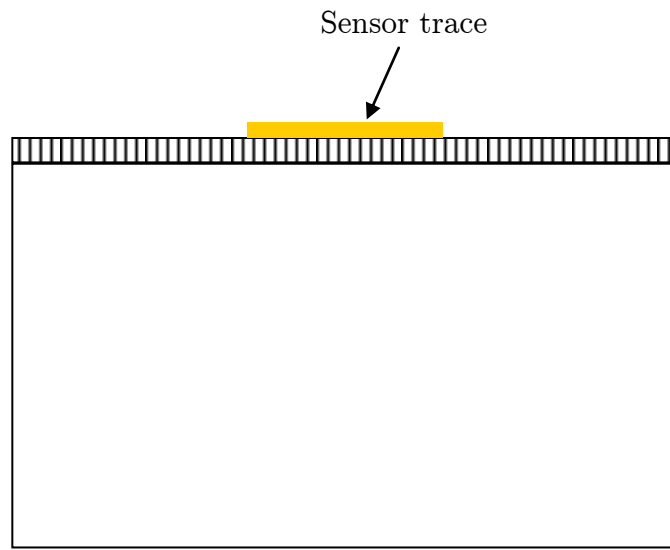


Figure 3.25 : Developed photoresist and Ti/Pt/Au deposition



**Figure 3.26** : Wafer with sensor trace.

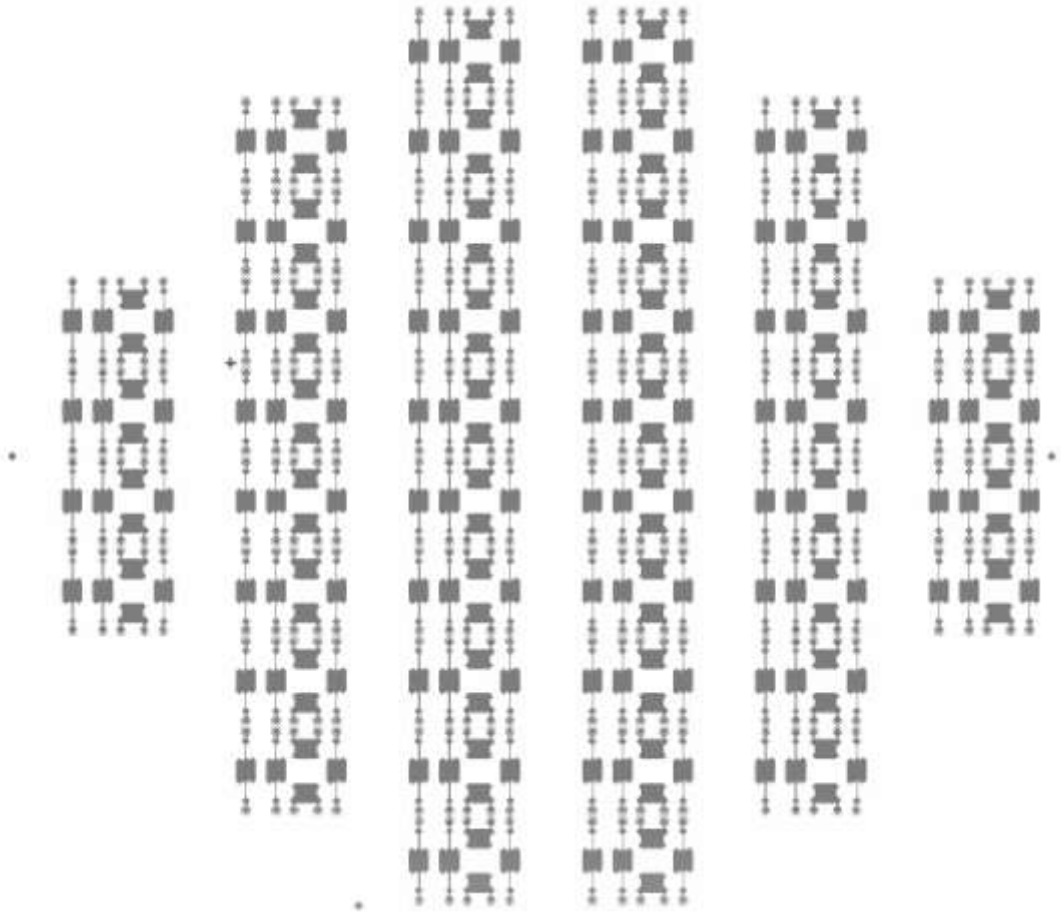
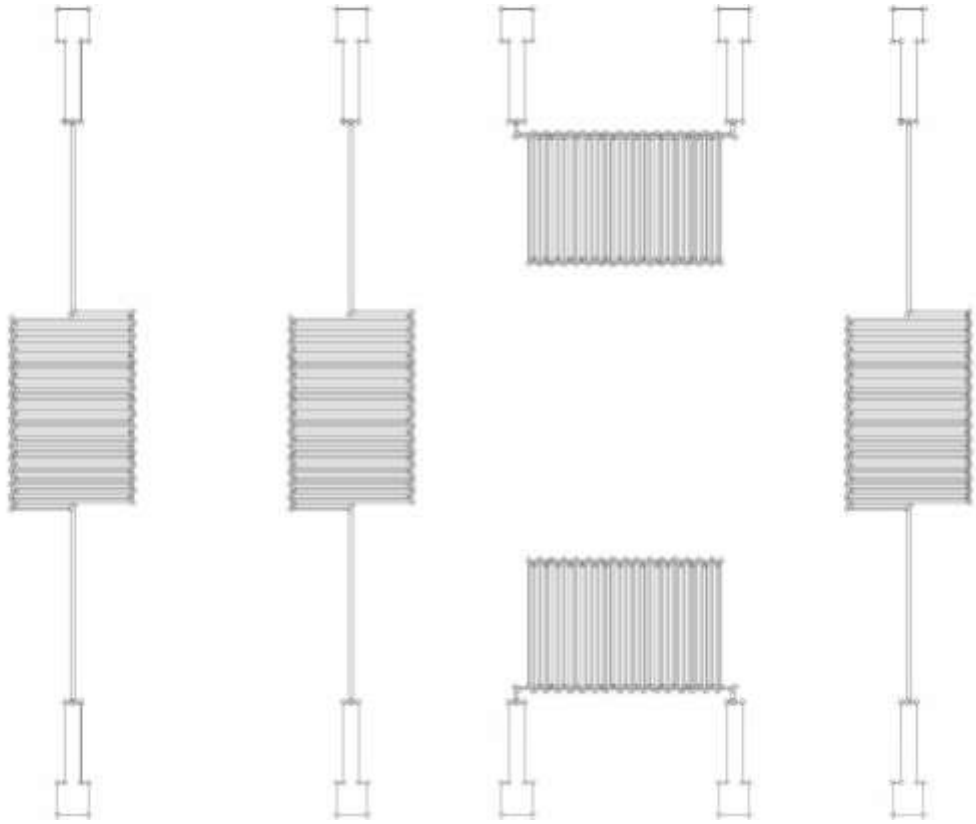
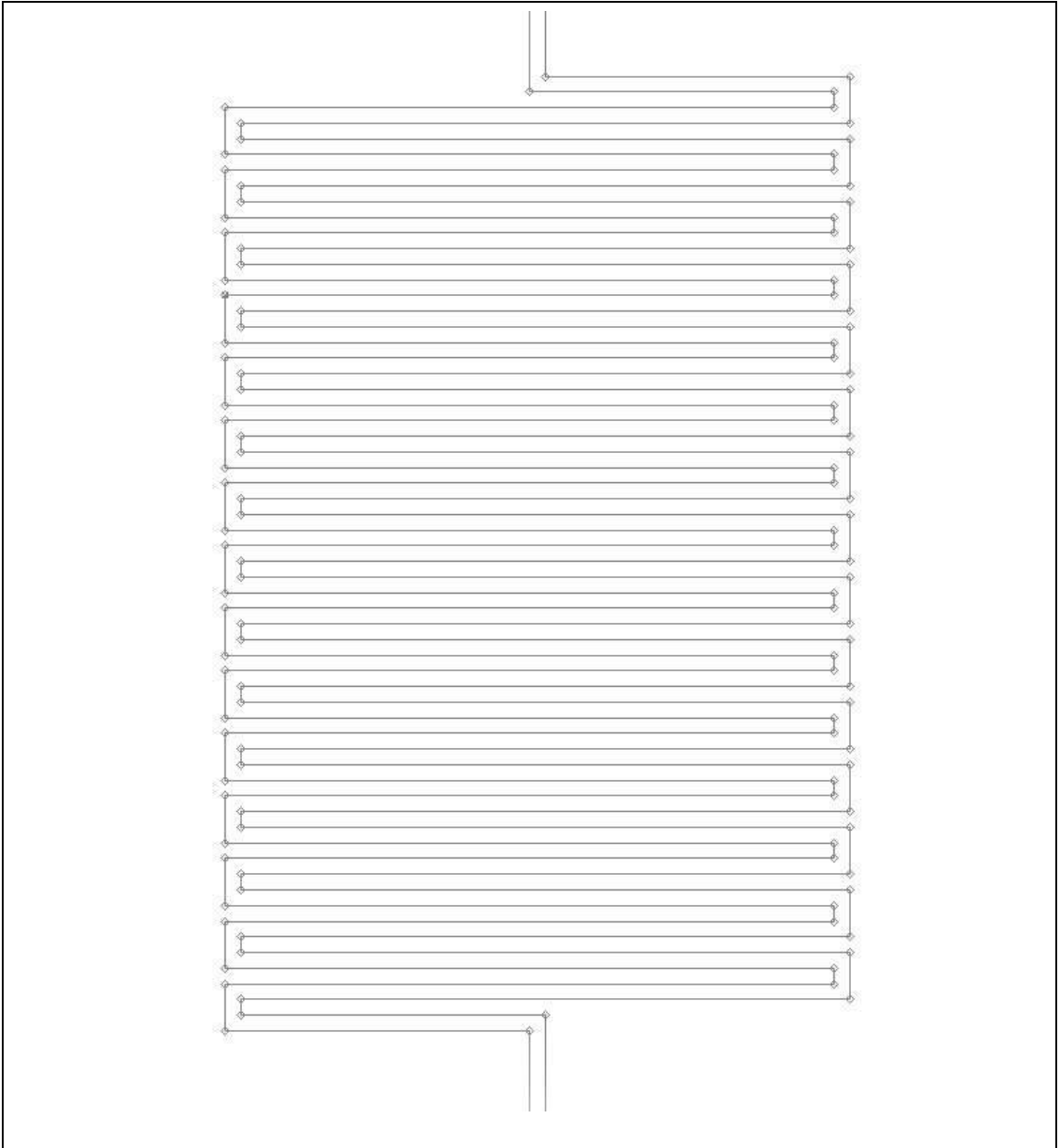


Figure 3.27 : Sensor mask (5 sensors per die)



**Figure 3.28** : Single die (5 sensors)





**Figure 3.29** : Sensor serpentine

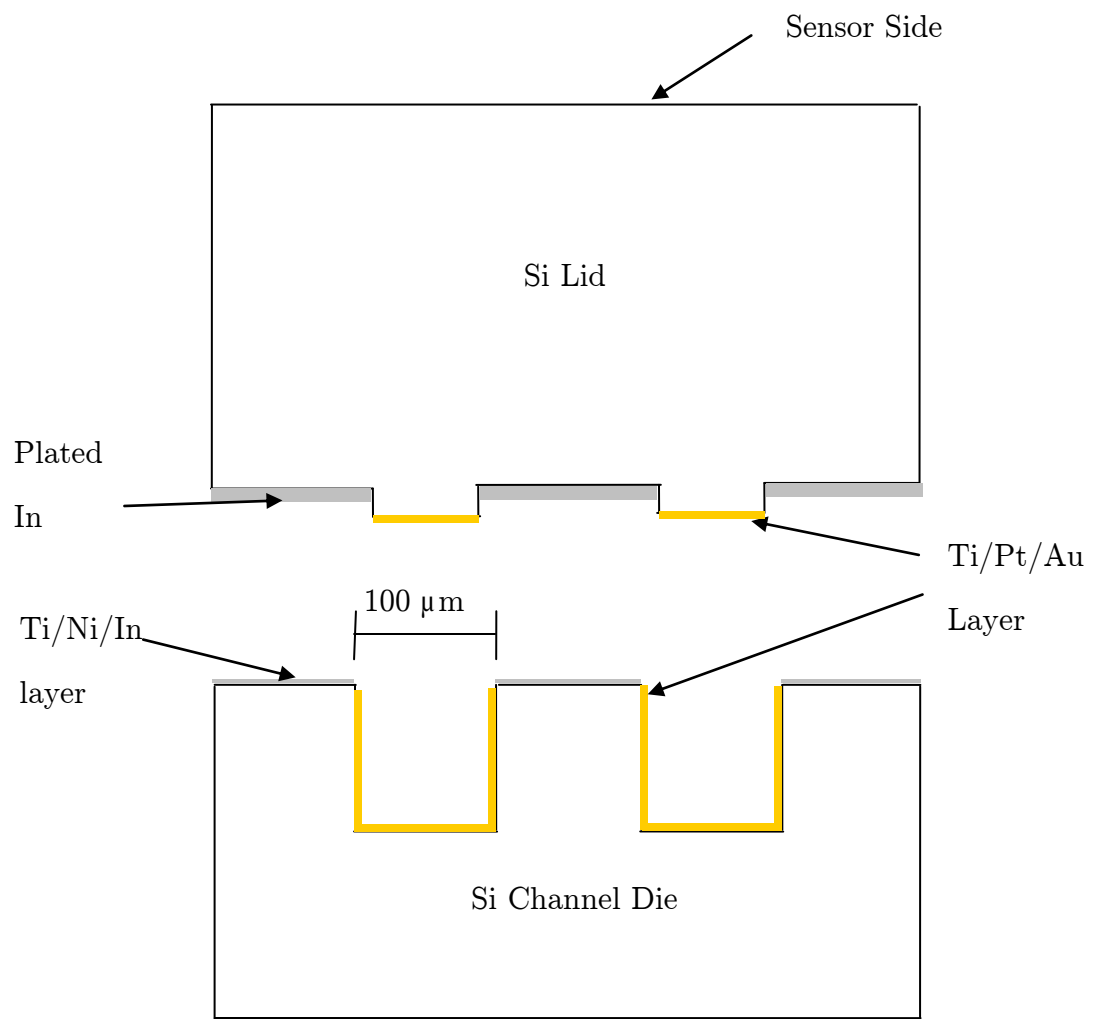


**Figure 3.30** : Final assembly

## CHAPTER 4

### TESTING AND RESULTS

#### 4.1 Introduction

In this chapter we will discuss the charging, sealing and testing procedure and have a look at the test results. The tests were carried out in the CAVE lab using the COMPIX infra red camera system.

#### 4.2 Charging

The micro heat pipes must be charged with right amount of fluid: too much results in flooding of the pipes and not enough leads to a dry out [26]. In our test, we used two fluids: de-ionized water and mercury, each of which required different charging. Testing was also done on a silicon dummy to compare the working of the above two micro heat pipes.

##### 4.2.1 Charging of Mercury

Mercury, a liquid at room temperature, is normally a non wetting liquid metal and is therefore, hard to put in the channels. Micro pipettes and micro pump were used to put mercury in the channels.

A syringe with mercury in it was mounted on the RAZEL™ micro pump and a rubber tube was attached to the syringe. The other end of the rubber tube was put over the micro pipette; the tip of which was less than 100 microns and easily fit into the channels. The whole system was kept on a THE MICRO MANIPULATOR COMPANY CORPORATION'S micro probe station. The micro

pipette was attached to one of the probes on the probe station for easy and precise movements of the micro pipettes. The pipettes were delicate and hence required precise movement in order to avoid breaking the tips. Fig 4.1 shows the setup used to fill the micro heat pipes with mercury. Fig 4.2 illustrates shows how mercury was put in the channel.

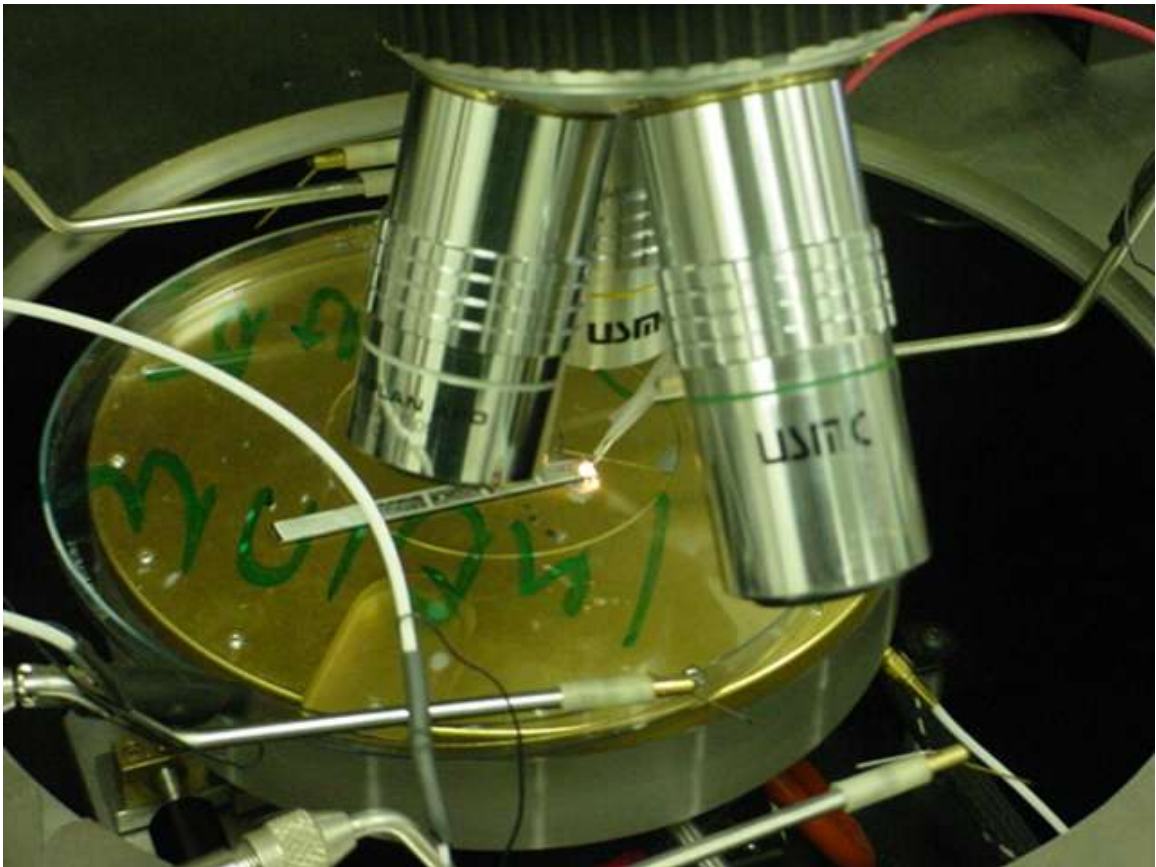


**Figure 4.1:** Setup used to fill micro heat pipes. The picture shows a test dummy being filled.

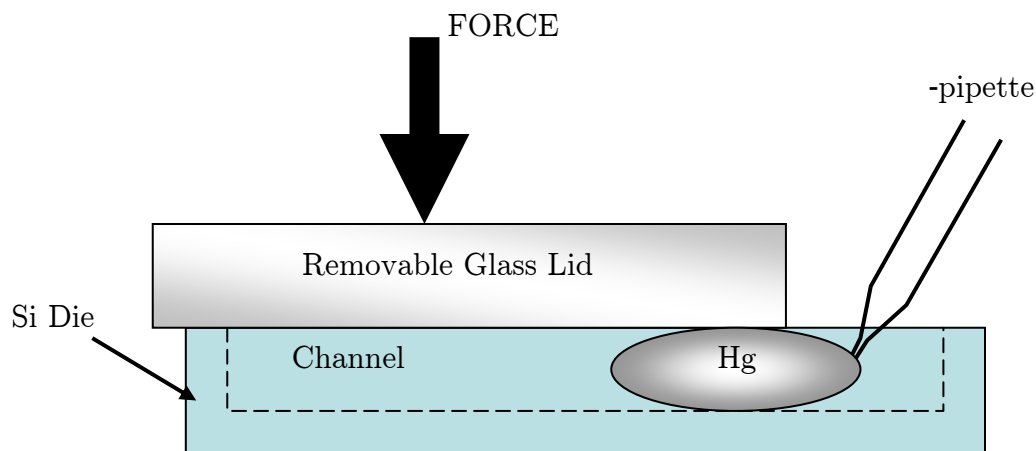


**Figure 4.2 :** Filling of Mercury in the channels

A micro heat pipe die with indium on the top surface of the walls and gold in the channels was cleaned with acetone and dried. A glass lid of the same size as the die was taped onto it, positioned such that there was a gap left for the micro pipette to go in the channels (as shown in fig 4.2). This assembly was then taped onto a Petri dish, which was then placed on the chuck of the probe station and vacuum was put on. This helped position and secure the die, not allowing it to move while we filled the channels.

After positioning the die and the micro pipettes, the syringe was gently squeezed by the micro pump. We monitored the progress of the mercury on the TV screen attached to the micro scope of the probe station (fig. 4.3). Once the mercury entered the channels, the syringe was pulled back, and the micro pipette was removed from the channel. Similar methods were followed for all 22 channels each die. The die was then covered and kept idle for some time (typically overnight) so

the mercury could consume the gold and start wetting the platinum. The die and the glass lid were then removed from the Petri dish and separated.



**Figure 4.3:** TV screen attached to microprobe station showing mercury in the channels.

#### 4.2.2 Charging of water

Charging the water was much simpler than charging the mercury because water doesn't have wetting issues. The water easily entered the micro heat pipes and stayed in the channels.

A die with channels was placed a in a beaker containing 15:1 solution of water and BRANSON OR formulated cleaning concentrate, for 2 minutes. The die was then taken out and squirted with acetone and dried, after which the channels

were charged with a small amount of de-ionized water. In the initial testing the amount of charge was not controlled so the charging percentage of charge varied for both mercury and water.

### **4.3 Sealing**

Sealing is usually done in vacuum to eliminate the channels of air and gases and ensure a leak proof system. A leak proof system allows for proper working of the micro heat pipes.

#### **4.3.1 Cleaning of lids**

In order to form a perfect bond, we needed to remove all the oxide from the indium surface of the lids. To achieve this, the lids were thoroughly cleaned just before using them on the micro heat pipes dies. The lids were dipped in 1:5 solution of HCL and water for one minute then the removed and squirted with acetone and dried.

#### **4.3.2 Sealing of mercury micro heat pipes**

The procedure used for mercury was simple. After the charging of mercury, the heat pipe die and lid were pressed against each other. The alignment was done visually since there were some allowable tolerances on the sides. Once the lid was pressed against the channels, the enclosed rectangular channels became pipes.

The lid and die were clamped with the help of a crocodile clip. The clip was held open with the help of a screw driver then dipped in liquid nitrogen to freeze it. Once the clip was frozen, it was removed and the micro heat pipes die was kept in it and the whole system was kept in a vacuum chamber for 24 hours. The entire assembly of clip and micro heat pipes is schematically shown in fig 4.4. Fig. 4.5 shows a schematic diagram of the vacuum chamber used to seal the micro heat

pipes. The clip was frozen so it would start clamping after some time and allow the pipes to be evacuated. After taking the micro heat pipes out of the vacuum chamber, they were kept in the oven for 20 minutes at 120°C to properly bond the lids to the die.

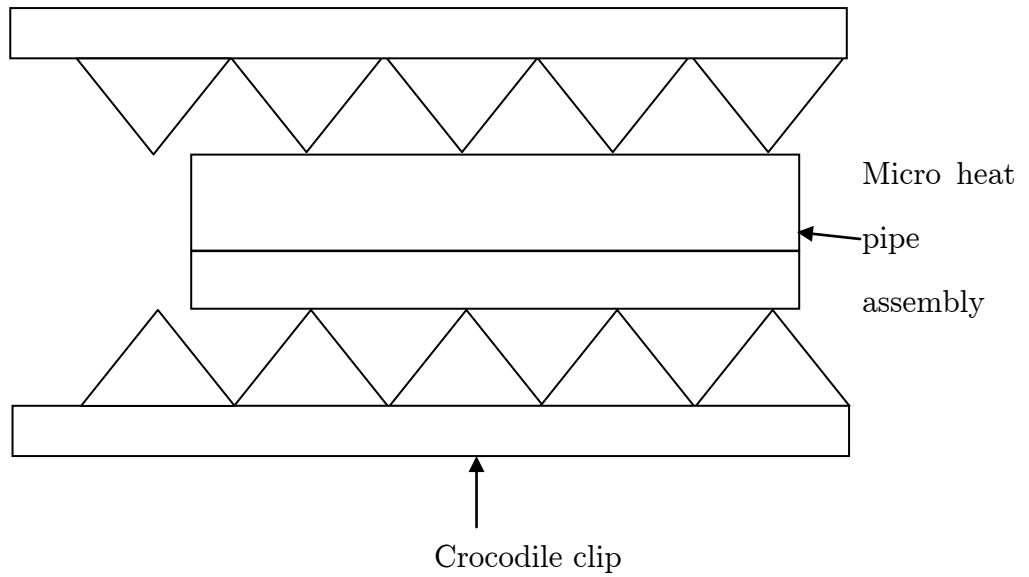
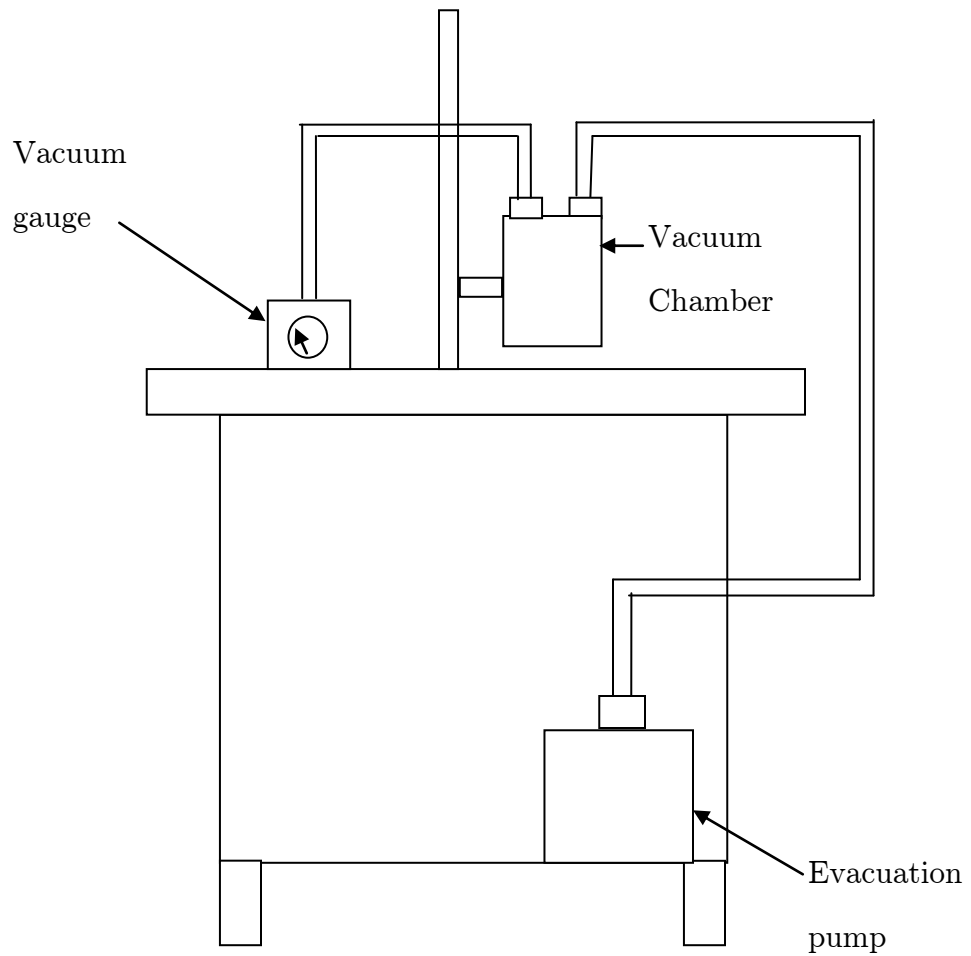


Figure 4.4 : crocodile clip and micro heat pipes.





**Figure 4.5:** Vacuum chamber used to seal the micro heat pipes

### 4.3.3 Sealing of water micro heat pipes

A very similar procedure was followed for the water filled micro heat pipes, except that after charging the micro heat pipes with water, the die was dipped in liquid nitrogen to freeze the water, forcing the water to stay in the pipes.

#### 4.3.4 Bonding technique used

Indium cold welding techniques are usually used in macroworld when two sufficiently thick, clean indium-coated surfaces are brought into contact at room temperature and held together by applying some pressure [27].

We tried the same method on micro heat pipes since indium does not readily react with mercury [27] and, hence, pose no danger of reaction in the device. In the micro fabrication process, one surface was deposited by a 1-micron thick-indium layer using an e-beam deposition machine and the other surface was plated with a 10 micron-thick indium layer giving us sufficiently thick indium layers on either surface for bonding.

During the bonding process, it is very important to ensure the cleanliness of the surfaces. An indium-coated surface readily reacts with oxygen and forms indium oxide on it; this oxide layer must be removed. If the layer is thick, the oxide can be removed chemically, but for thin layers chemicals cannot be used since they tend to remove the indium layer, too [27].

In our procedure, the oxide on the plated surface was removed by chemicals such as HCL, and the oxide on the deposited layer was removed with the help of the BRANSON solution. Both surfaces were brought in contact as quickly as possible so a new oxide layer could not form on the Indium surfaces.

#### 4.4 Testing

We performed several tests to check the working feasibility of the micro heat pipes. Heat was produced with the help of NiCr and tungsten wires, and the temperatures were measured with the help of IR camera. The sensors fabricated on the lids were not used since their calibration results were not reproducible. But the sensors were used as reference points while looking under the IR camera. The

temperatures at sensor 1 and sensor 5 locations were recorded. The distance between the centers of both the sensors was 5500  $\mu\text{m}$ .

#### 4.4.1 Board

The boards shown in fig. 4.6, were used for support and to connect the sensors on the lids to an area where the resistance could be measured. They were made up of Liquid Crystal Polymer (LCP). LCP was chosen because it could be etched and was easily available.

The LCP had copper on both sides. Initially, the copper was wet-etched to form the traces on the board for connections, and the LCP was through etched (DRY) to form a hole for placing the micro heat pipes. This hole had copper on its back.

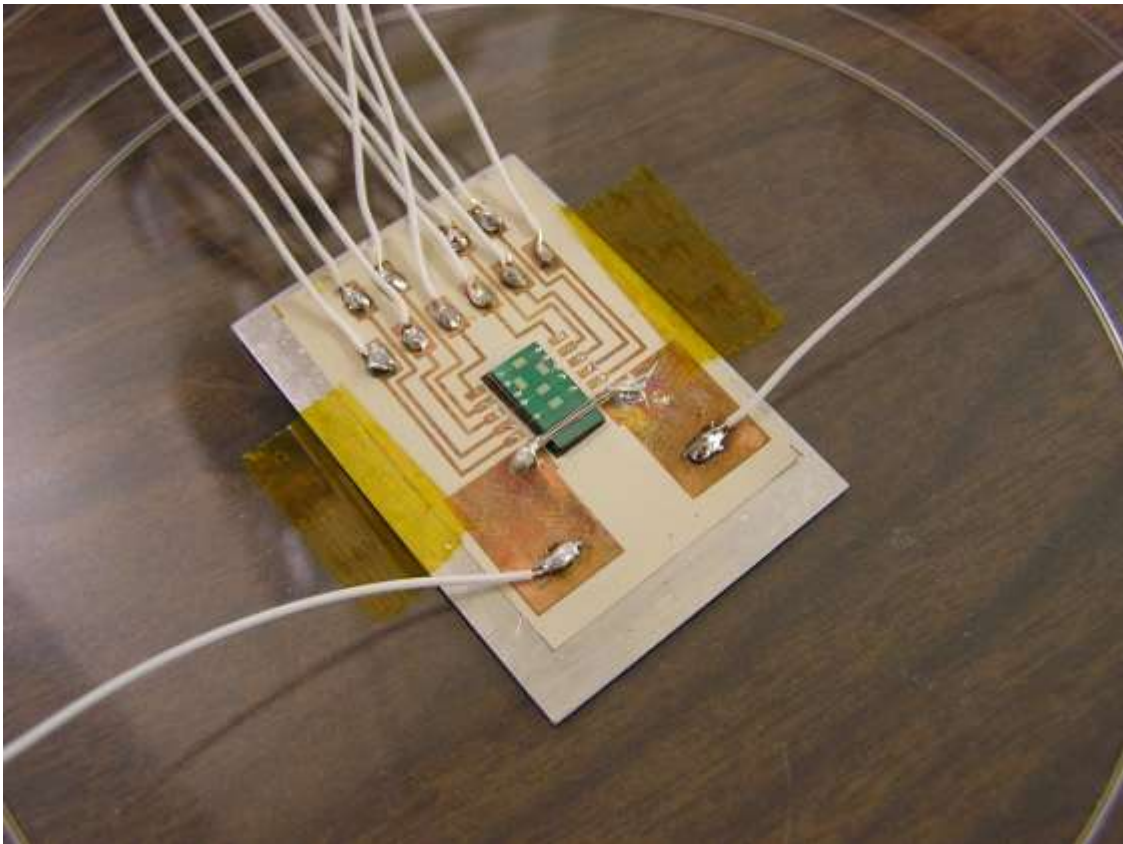


**Figure 4.6** : LCP board with micro heat pipes and lead and heating wires on it.

#### 4.4.2 Experiments

Experiments were carried out in the CAVE lab under an infra red camera.

Figure 4.6 shows the experimental setup along with IR camera.

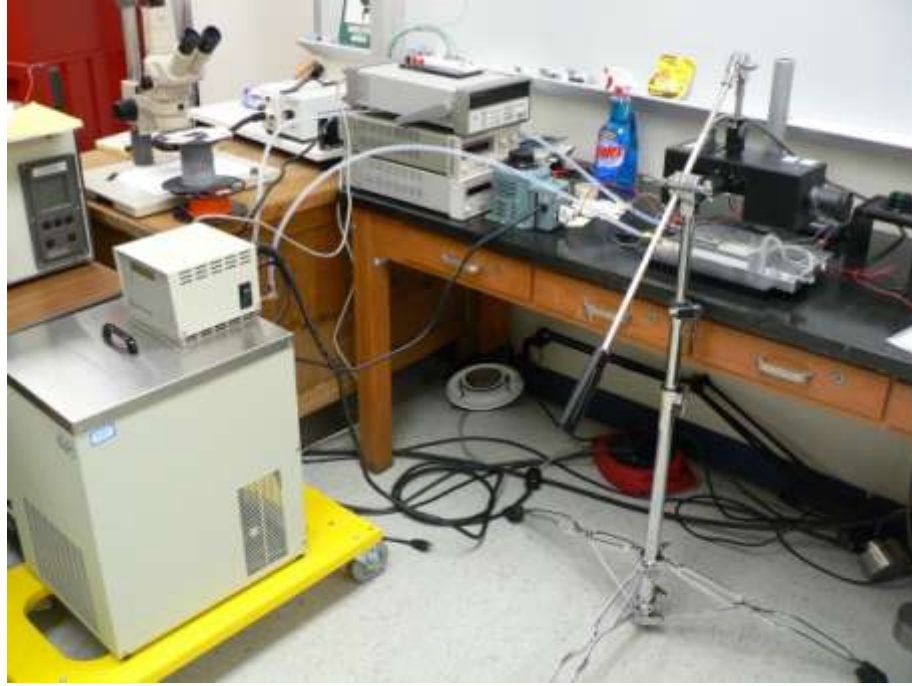


**Figure 4.7** : Experimental setup

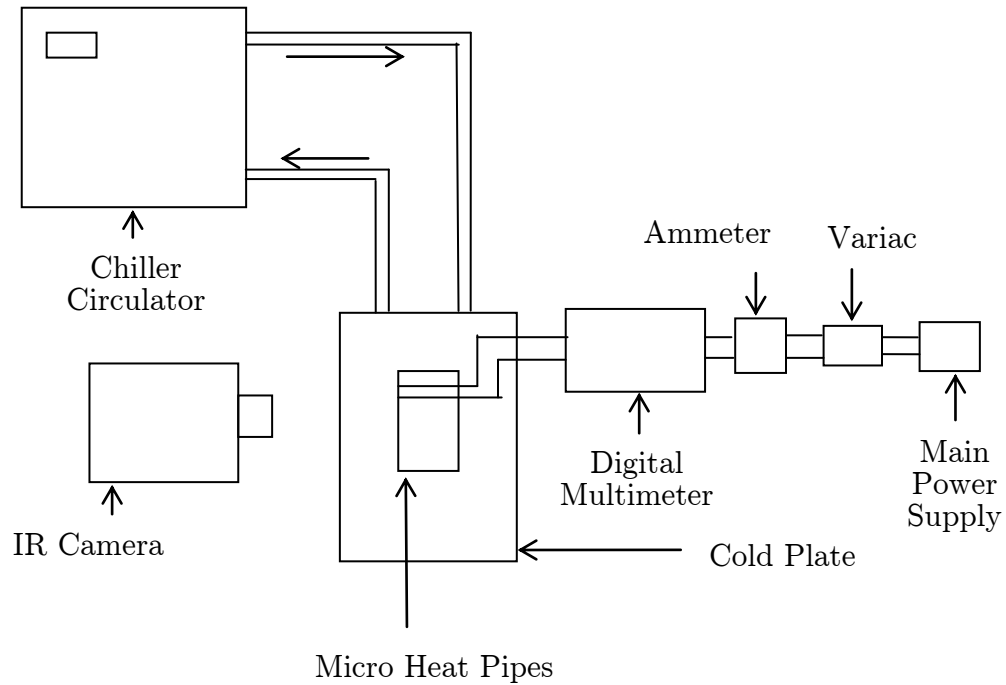


**Figure 4.8 :** Schematic Diagram of testing apparatus

The LCP board, with the micro heat pipe system attached to it, was glued to an aluminum or copper board to give itself stability. Thermal grease was then used to secure the whole assembly on the cold plate which had an inlet and outlet through which water at room temperature was passed with the help of FISHER SCIENTIFIC'S Isotemp 1013D chiller.

Power to the heating wire was provided with the help of SUPERIOR powerstat variable transformer. The current was measured by an ammeter and voltage was measured by a multi meter.

We tested three different samples: one was a simple silicon piece in the shape of the sample; another was water-filled micro heat pipes and the third was mercury-filled micro heat pipes.

#### **4.4.3 Results**

The results for si dummy, water-filled micro heat pipes and mercury-filled micro heat pipes are shown in three different tables. IR image for one of the readings is provided, which elaborates the way readings were taken. T1 was the temperature recorded by or seen under the IR of sensor 1, which was near to the wire. T5 was the temperature recorded by or seen under the IR of sensor 5, which was near the end of the micro heat pipe. Fig. 4.9 shows the numbering of the sensors. All the collected data is represented in three separate graphs for mercury filled micro heat pipes, water filled micro heat pipes and silicon dummy. The graphs are plotted power against temperature difference (T1-T5). Finally comparable results are tabulated and a graph for the following is shown.

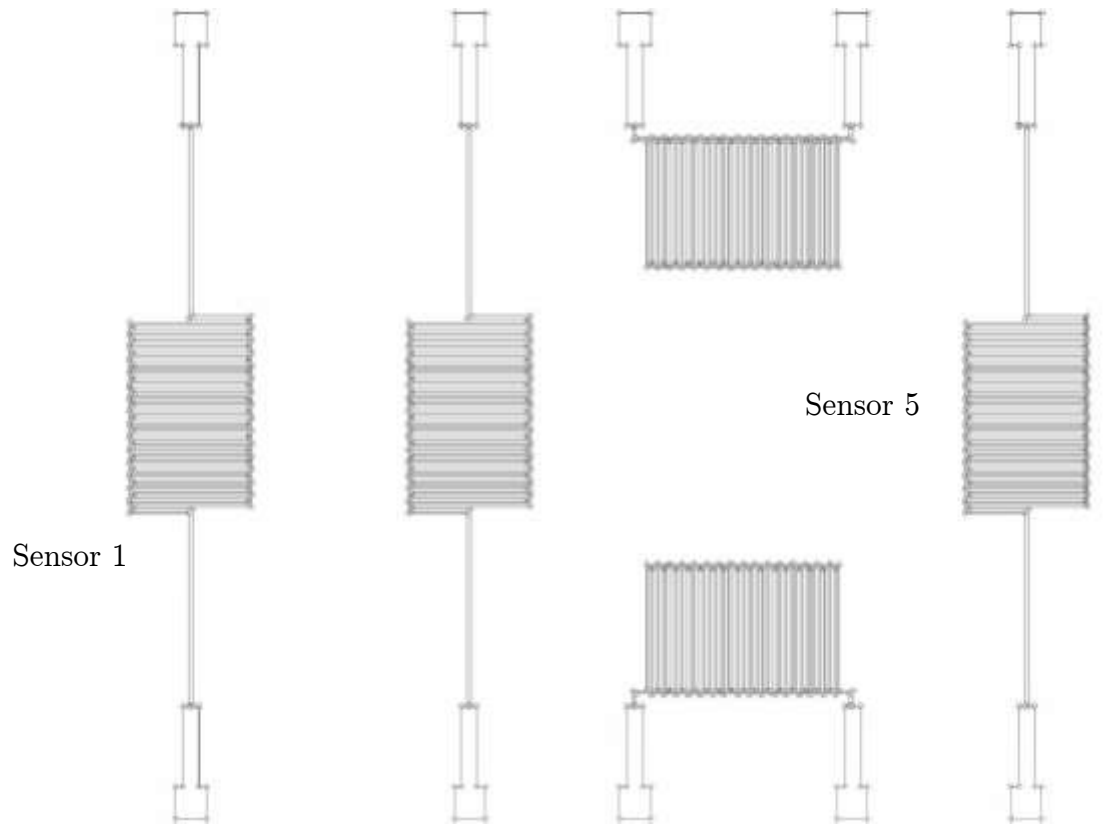


**Figure 4.9 :** Numbering of the sensors

#### 4.4.3.1 Silicon dummy

Power (W)	T1 (C)	T5 (C)	T1-T5 (C)
0.07	23.3	22.5	0.8
1.26	25.1	28.4	-3.3
1.32	28.6	23.6	5.1
2.37	25.9	23.6	2.3
2.53	27.1	25.3	1.8
2.59	45.2	24.9	20.3
5.11	31.8	26.6	5.2
5.33	33.9	27.3	6.6
5.98	92.1	30.2	61.9
6.08	37.4	28.4	9.0
7.22	47.1	39.3	7.8
9.25	48.4	33.9	14.6
14.60	69.0	39.0	29.9

**Table 4.1:** Test results for Si dummy



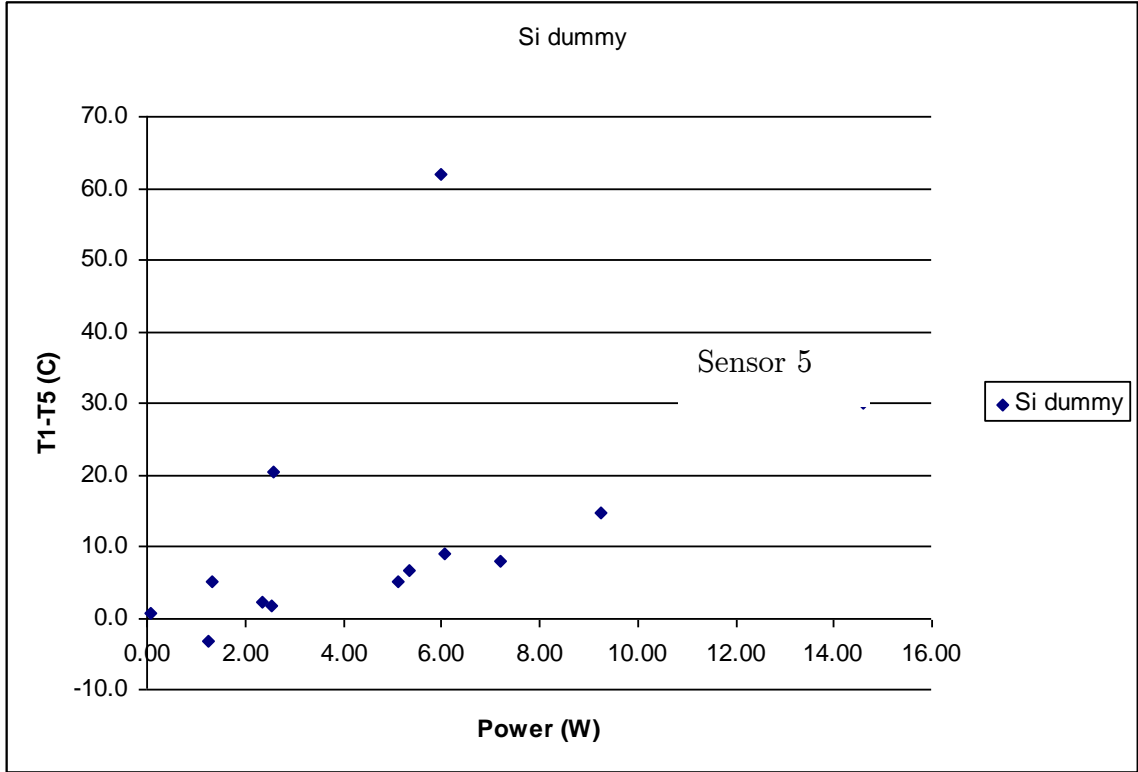


Figure 4.10 : Graphical representation of Si dummy results

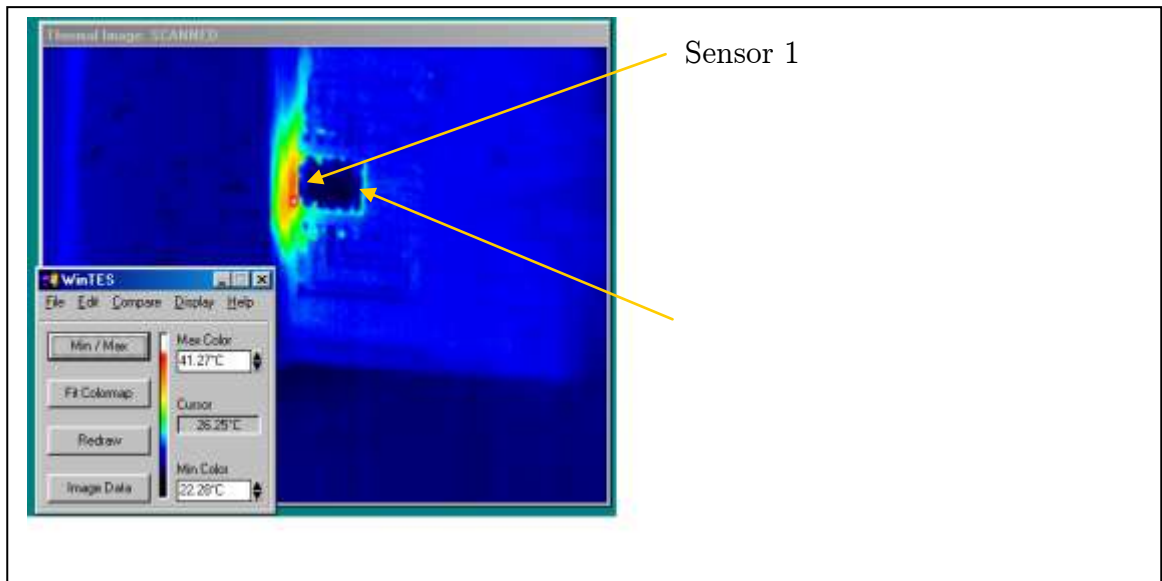


Figure 4.11 : Infra red image of micro heat pipes at a power of 2.37 W.

#### 4.4.3.2 Water-filled micro heat pipes

Power (W)	T1 (C)	T5 (C)	T1-T5 (C)
2.35	30.8	28.0	2.8
4.79	38.4	39.3	-0.9
7.53	52.1	46.0	6.1
9.90	62.2	52.7	9.5
12.17	75.6	54.1	21.5
15.45	94.6	65.5	29.2

Table 4.2 : Test results for water-filled micro heat pipes

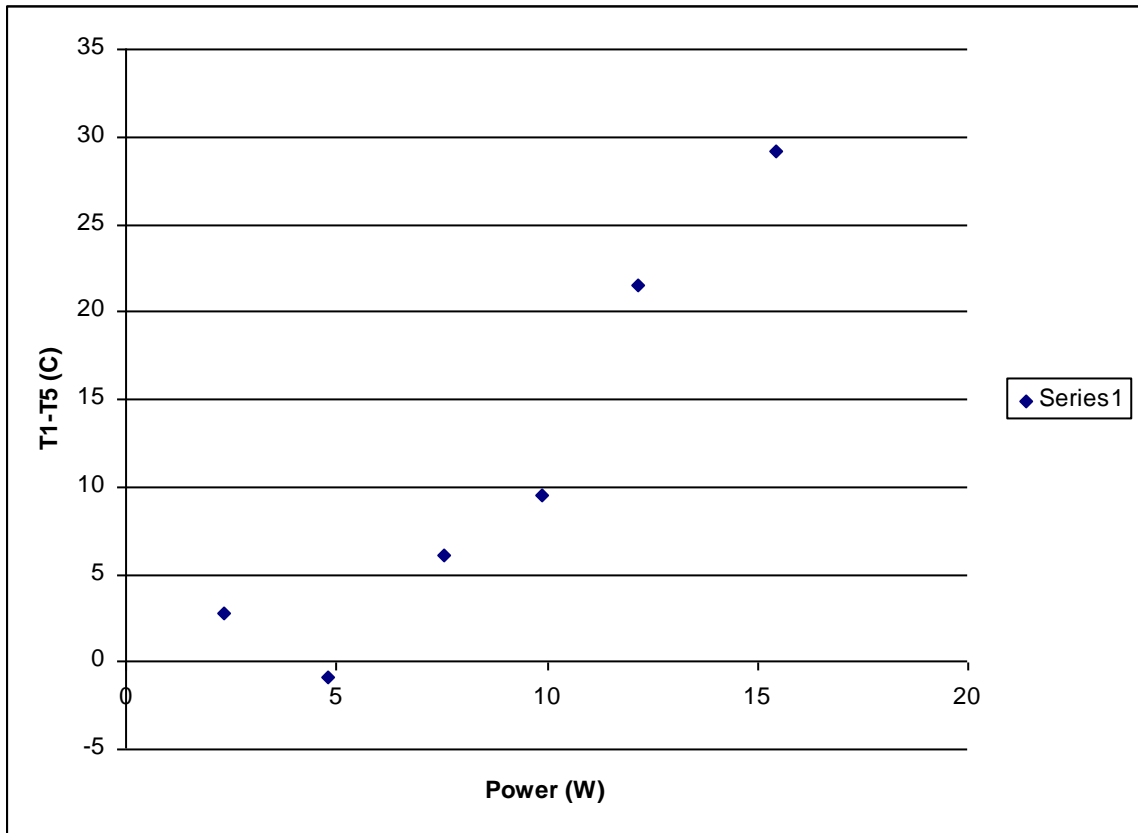


Figure 4.12 : Graphical representation of water-filled micro heat pipes

#### 4.4.3.3 Mercury-filled micro heat pipes

<b>Power (W)</b>	<b>T1 (C)</b>	<b>T5 (C)</b>	<b>T1-T5 (C)</b>
0.36	22.0	21.5	0.5
0.64	20.5	21.8	-1.3
1.02	24.5	23.9	0.5
1.34	35.0	27.8	7.2
1.57	22.4	23.4	-1.0
1.88	27.0	26.1	0.9
2.31	25.7	24.8	0.9
2.51	24.7	23.8	0.9
2.88	42.4	28.6	13.8
2.91	27.1	27.9	-0.7
3.04	32.4	30.9	1.5
4.29	49.4	29.1	20.3
5.01	30.2	30.7	-0.5
5.06	26.1	26.8	-0.7
5.62	36.6	27.2	9.4
5.66	68.3	30.7	37.6
7.58	80.1	31.6	48.5
7.79	41.9	39.0	2.8
7.95	36.8	34.0	2.8
9.64	61.7	30.2	31.5
10.08	41.0	37.2	3.8
10.08	41.6	39.5	2.1
10.75	38.2	35.0	3.2
14.68	59.2	48.7	10.5

17.47	61.3	46.3	15.1
-------	------	------	------

**Table 4.3 :** Test results for mercury-filled micro heat pipes

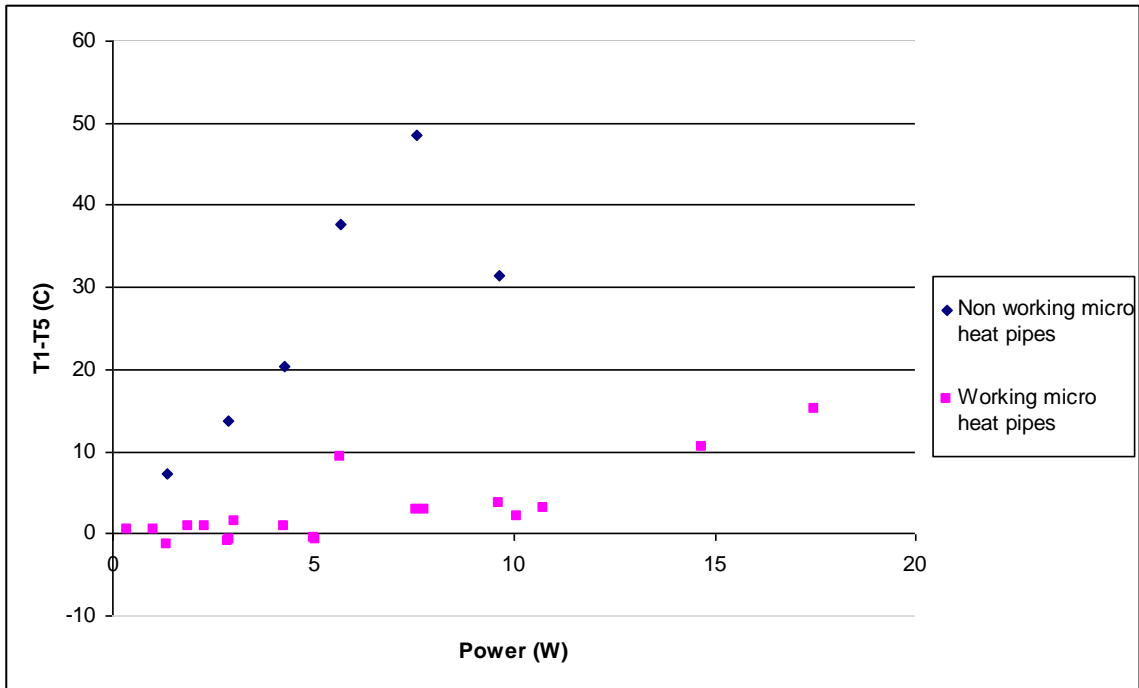


**Figure 4.13 :** Graphical representation of mercury-filled micro heat pipes

#### 4.4.4 Conclusion

Power (+/- 0.51 W)	T1-T5 for Si dummy (C)	T1-T5 for water filled micro heat pipes (C)	T1-T5 for mercury filled micro heat pipes (C)

7.5	7.8	6.1	2.8
9.5	14.5	9.5	3.8
15	29.9	29.2	10.5

**Table 4.4 :** Comparable results

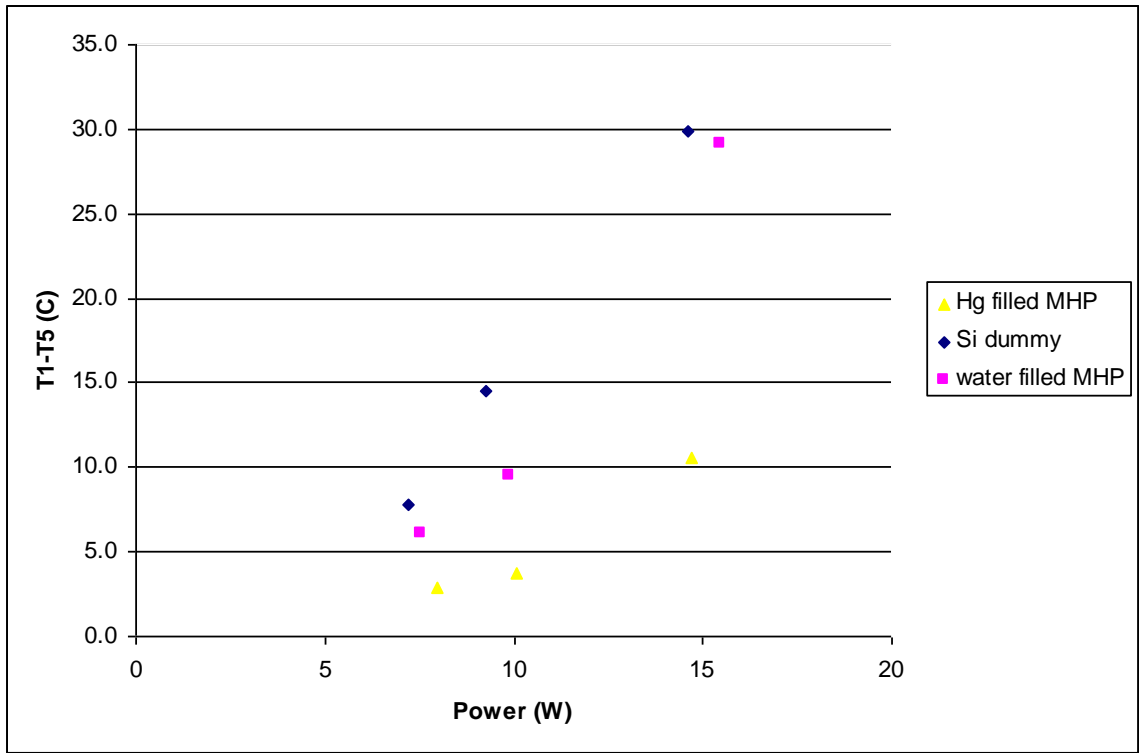


**Figure 4.14 :** Graphical representation of the comparable results

The results showed that the dies with mercury filled micro heat pipes and water filled micro heat pipes required lower temperature difference ( $T_1-T_5$ ) to transport approximate same amount of power as compared to Si dummy die. This indicated increase in thermal conductivity of the die when mercury and water filled micro heat pipes were used. The graph showing distribution of mercury filled micro heat

pipes (fig. 4.11) also show readings from a non working micro heat pipes. The tests were also useful in concluding that mercury can be used as a working fluid in a micro heat pipe.

## CHAPTER 5

### DISCUSSION

#### 5.1 Overview

In this work, micro heat pipes arrays were fabricated on a silicon wafer and tested. Two different working fluids were used in these micro heat pipes. One of them was DI water and the other one was mercury. The dimensions and geometries of the micro heat pipes were same. A silicon dummy was also tested along with micro heat pipes to compare the results. Fabrication method was discussed in details and results were shown. Fabrication was done using micro fabrication techniques and the micro heat pipes were sealed using Indium cold welding procedure. This sealing method helped in using liquid metals such as mercury and also helped in achieving sealing without use of high temperatures. The heat pipes were tested to see whether the micro heat pipe arrays worked and whether the sealing hold good. The micro heat pipes were not tested to see the performance since the charging method used was not accurate.

Micro heat pipes are an emerging technique and lot of work has been done in recent years to study its use in variety of applications from high power generating electronics to brain surgery. However, the work done so far mainly discussed DI water, methanol and refrigerants as working fluids. Very few have explored the possibility of using liquid metals as a working fluid. The literature review done suggests that though people have used models to predict the performance of a mercury micro heat pipes, rarely people have tried to fabricate them and perform experiments on them. The main reasons being the wetting issue

and sealing problems related with using mercury as a working fluid. In the above work the wetting issues were taken care of by using gold as a sacrificial layer letting mercury wet platinum in its purest form [24]. Good sealing was achieved by using cold indium welding [27].

The tests carried on mercury filled micro heat pipes showed good indications that the micro heat pipes were working. Being a liquid metal, mercury has a very good heat carrying capacity. It also has a good working range. However filling of mercury into the channels is difficult.

## **5.2 Future work**

Fabrication procedure should be standardized so as to get more yields from a single wafer. Yield is the amount of good and working dies from a single wafer. Standardizing will also help in getting large amount of lids with working sensors on it.

More advance techniques should be used to fill and evacuate the micro heat pipes. This would help in controlling the charge that is being put into the micro heat pipes. Literature review shows that the performance of micro heat pipes is dependent on the amount of charge.

It is recommended that the testing methods should be changed in order to reduce heat loss to the environment. Also temperature measurement can be done more accurately. This would help in accurately determining the performance of micro heat pipes. This work is currently in focus at the AuTherMM Laboratory in Auburn University.



## BIBLIOGRAPHY

- [1] A. Faghri, *Heat Pipe Science and Technology*. Washington, DC: Taylor & Francis, 1995.
- [2] B. B. F.M GERNER, H.T.HENDERSON and P.RAMADAS, "Silicon-Water Micro Heat Pipes," 1993.
- [3] G. P. Peterson, *An Introduction to Heat Pipes: Modelling, Testing, and Applications*. New York, NY: John Wiley & Sons, Inc., 1994.
- [4] A. F. Yiding Cao, E. Thomas Mahefkey, "Micro/Miniature Heat Pipes and Operating Limitations," *Heat Pipes and capillary Pumped Loops*, vol. 236, 1993.
- [5] S. L. M Le Berre, V Sartre, M Lallemand, "Fabrication and experimental investigation of silicon micro heat pipes for cooling electronics," *Journal of Micromech, Microeng.*, vol. 13 (2003), pp. 436-441, 2003.
- [6] J. M. A. Bassam Badran, Frank M. Gerner, Padmaja Ramadas, H. Thruman Henderson, Karl W. Baker, "Liquid-Metal Micro Heat Pipes," *Heat Pipes and capillary Pumped Loops*, vol. 236, 1993.
- [7] K. D. Youngcheol Joo, Chang-Jin Kim, "Fabrication of Monolithic Microchannels for IC chip cooling."
- [8] M. W. Man Lee, Yitshak Johar, "Integrated Micro-Heat-Pipe Fabrication Technology.," *Journal of Microelectromechanical Systems.*, vol. 12, pp. 138-146, 2003.
- [9] M. W. Man Lee, Yitshak Johar, "Characterization of an integrated micro heat pipe," *Journal of Micromech, Microeng.*, vol. 13, pp. 58-64, 2002.
- [10] G. P. P. Arnab K. Mallik, Mark H. Weichold, "Fabrication of Vapor-Deposited Micro Heat Pipe Arrays as an integral part of semiconductor devices," *Journal of Microelectromechanical Systems.*, vol. 4, pp. 119-131, 1995.
- [11] G. P. P. Y.X.Wang, "Analysis of wire bonded micro heat pipes," *Journal of thermophysics and heat transfer*, vol. 16, pp. 346-355, 2002.
- [12] S. M. Wai Y. Liu, Linda P. B. Katehi, Hamed Khalkhali and Katsuo Kurabayashi, "Polymer Micro-heat-pipe for InP/InGaAs technologies.

- [13] S.-H. T. Shung-Wen Kang, Hong-Chin Chen, "Fabrication and test of radial grooved micro heat pipes," *Applied Thermal Engineering*, pp. 1559-1568, 2002.
- [14] A. B. D. G.P.Peterson, M.H.Weichold, "Experimental Investigation of Micro heat pies fabricated in Silicon wafers," *journal of Heat Transfer, Transactions ASME*, vol. 115, pp. 751-756, 1993.
- [15] V. S. S.Launay, M.Lallemand, M.B.H.Mantelli, Kelber Vieira de Paiva, "Investigation of a micro heat pipe array," *International Journal of Thermal Sciences*, pp. 499-507, 2003.
- [16] D. H. Shung-Wen Kang, "Fabrication of star grooved and rhombus grooves micro heat pipes.," *Journal of Micromechanics and Microengineering*, pp. 525-531, 2002.
- [17] Y. L. W.Kinzy Jones, Mingcong Gao, "Micro Heat Pipe in Low Temperature Cofire Ceramic (LTCC) Substrates.," *IEEE TRANSACTION ON COMPONENTS AND PACKAGING TECHNOLOGIES.*, vol. 26, pp. 110-115, 2003.
- [18] G. P. P. D.Wu, W.S.Chang, "Transient experimental investigation of micro heat pipe," *Journal of thermophysics and heat transfer*, vol. 5, pp. 539-544, 1991.
- [19] A. L. C.Gillot, M.Ivanova,.Y.Avenas, C.Schaeffer, E.Fournier, "Experimental study of a flat silicon heat pipe with microcapillary grooves," presented at 2004 Inter Society Conference on thermal phenomena, 2004.
- [20] R. Ponnappan, "A novel Micro-capillary Groove-wick Miniature Heat Pipe," presented at 35th Intesociety Energy Conversion Engineering Conference., 2000.
- [21] K. P. Hallinan, Bhagat, Wilber, Kashaboina, Balamurali, Kashani, A.Reza, "Electro-hydrodynamic augmentation of heat transport in micro heat pipe arrays.," presented at Proceedings of the 1998 ASME international mechanical engineering congress and exposition., Anaheim, Ca, USA, 1998.
- [22] L. M. P. Laura J. Meyer, "Fabrication of a Silicon-Carbide Micro-Capillary Pumped Loop for Cooling High Power Devices.," presented at Itherm 2004 - Ninth Intersociety Conference on Thermal & Thermomechanical Phenomena in Electronic Systems., Las Vegas, NV, 2004.
- [23] R. C. Jager, *INTRODUCTION TO MICROELECTRONIC FABRICATION*, vol. V, Second ed: Prentice-Hall.
- [24] A. D. F. Hongjun Zeng, Ziliang Wan, Pancham R. Patel, "Piston-motion micromirror based on electrowetting of liquid metals.," *Journal of Microelectromechanical Systems.*, vol. 14, pp. 285-294, 2005.
- [25] "SemiconTimes."
- [26] V. S. S.Launay, M.Lallemand, "Experimental study on silicon micro heat pipe arrays," 2003.

- [27] R. D. Daniel Harris, Omkar Nadgauda, Nicole Sanders, Charles Ellis and Mike Palmer, "A packaging Sealing Technique for Mercury Filled Microfluidic Devices," presented at IMAPS, Scottsdale, Arizona, 2006.
- [28] J. R. Taylor, *An Introduction To Error Analysis*, Second ed.